^{15}N and ^{13}C NMR Studies of the Interaction of Cyanide Ion With Gold(I) Drugs

by

Ibrahim Hamed Ghazi

A Thesis Presented to the

FACULTY OF THE COLLEGE OF GRADUATE STUDIES

KING FAHD UNIVERSITY OF PETROLEUM & MINERALS

DHAHRAN, SAUDI ARABIA

In Partial Fulfillment of the
Requirements for the Degree of

MASTER OF SCIENCE

In

CHEMISTRY

June, 1993

Order Number 1354042

^{15}N and ^{13}C NMR studies of the interaction of cyanide ion with gold(I) drugs

Ghazi, Ibrahim Hamed, M.S.

King Fahd University of Petroleum and Minerals (Saudi Arabia), 1993

U·M·I
300 N. Zeeb Rd.
Ann Arbor, MI 48106

^{15}N AND ^{13}C NMR STUDIES OF THE INTERACTION OF CYANIDE ION WITH GOLD(I) DRUGS

BY

IBRAHIM HAMED GHAZI

A Thesis Presented to the

FACULTY OF THE COLLEGE OF GRADUATE STUDIES

KING FAHD UNIVERSITY OF PETROLEUM & MINERALS

DHAHRAN, SAUDI ARABIA

In Partial Fulfillment of the
Requirements for the Degree of

MASTER OF SCIENCE

In

CHEMISTRY

JUNE 1993

RECEIVED 2 4 AUG 1993

KING FAHD UNIVERSITY OF PETROLEUM AND MINERALS
DHAHRAN 31261, SAUDI ARABIA

COLLEGE OF GRADUATE STUDIES

This Thesis, written by Ibrahim Hamed Ghazi under the direction of his Thesis Advisor and approved by his Thesis Committee, has been presented to and accepted by the Dean of the College of Graduate Studies, in partial fulfillment of the requirements for the degree of MASTER OF SCIENCE in Chemistry.

Thesis Committee

Dr. A.A. Isab
Thesis Advisor

Dr. Abdulrahman Al-Arfaj
Member

Dr. Herman Perzanowski
Member

Dr. Abdulrahman Al-Arfaj
Department Chairman

Dr. Ala A-Rabeh
Dean, College of Graduate Studies

Date 21st of Aug 93

This thesis is dedicated to my parents, wife
brother Saleh and my daughter Lojain

ACKNOWLEDGEMENTS

Acknowledgement is due to King Fahd University of Petroleum and Minerals for extending all facilities and providing financial support, and to the Chemistry Department and its chairman.

I would like to offer my indebtedness and sincere appreciation to my major advisor Dr. A. A. Isab, for suggesting the problem and for the great assistance in supervising and coordinating the whole work. My sincere thanks are to the other members of my thesis committee, Dr. A. Al-Arfaj and Dr. H. Perzanowski for their great help, guidance and suggestions.

Thanks are also extended to Mr.Farouqi for his help in glass blowing. Also I would like to thank Mr. M. Arab, Mr. M. Fahmi, and Mr. Mazhar for helping me to complete my experimental work.

TABLE OF CONTENTS

CHAPTER THREE

EXPERIMENTAL AND RESULTS

LIST OF TABLES

LIST OF FIGURES

THESIS ABSTRACT

NAME OF STUDENT : IBRAHIM HAMED GHAZI
TITLE OF STUDY : ^{15}N AND ^{13}C NMR STUDIES OF THE INTERACTION OF CYANIDE ION WITH GOLD DRUGS
MAJOR FIELD : INORGANIC CHEMISTRY
DATE OF DEGREE : JUNE, 1993

^{15}N NMR studies of the interaction of ^{15}N cyanide ion with gold(I)thiomalate (Autm) and gold(I)thioglucose (Autg) have been carried out at pH* 7.40. The chemical shifts of the two ^{15}N containing species $Au(C^{15}N)_2^-$ and RS-Au-$C^{15}N^-$ (where RS^-= tm^- or tg^-) were identified. From the broadened ^{15}N NMR signals, approximate lifetimes of the RS-Au-CN^- species were calculated.

Captopril (Hcap) with gold(I) forms a 1:1 *crystalline* complex Au(I)cap. The exchange reactions of thiomalate and cyanide with Au(I)cap have been studied using ^{13}C NMR spectroscopy. Au(I)cap forms a very high molecular weight polymer. Thiomalate and CN^- both bind to Au(I)cap, however, as expected, CN^- binds more strongly. Both the cis and trans Au(I)cap isomers were observed upon the addition of $^{13}CN^-$ to A(I)cap solution.

The ligand scrambling reaction of $R_3PAuC^{15}N$ to form $(R_3P)_2Au^+$ and $Au(C^{15}N)_2^-$ has been studied for R = Me, Et, i-Pr, and Ph. Two ^{31}P NMR resonances were observed for R_3PAuCN and $(R_3P)_2Au^+$ species. However, for the ^{15}N NMR, apart from $Et_3PAuC^{15}N$, where two resonances were detected, only one averaged resonances observed for $R_3PAuC^{15}N$ (R = Me, Ph).

MASTER OF SCIENCE DEGREE
KING FAHD UNIVERSITY OF PETROLEUM AND MINERALS
Dhahran, Saudi Arabia
June,1993

الخلاصة

إ سم الطالب :إ براهيم حامد غازي

عنوان الرسالة :دراسة تفاعل أيون السيانيد مع أدوية الذهب بإستخدام الرنين النووي المغناطيسي لعنصري نيتروجين-١٥وكربون-١٣

التخصص : كيمياء غيرعضوية

تاريخ الحصول على الدرجة : يونيو١٩٩٣م

لقد تم دراسة تفاعل أيون السيانيد المميز (-C1 5N) مع مركب ثيومالات الذهب(١) وثيوجلوكوزالذهب(١) بواسطة الرنين النووي المغناطيسي لعنصرالنيتروجين-١٥ في محاليل ذات رقم هيدروجيني (pH*) يساوي ٤ . ٧. وقد تم تحديد الإزاحة الكيميائية على مخطط طيف الرنين النووي المغناطيسي لمركبين ناتجين عن هذا التفاعل وهماثنائي سيانيد الذهب (-Au(CN)2) وثيولات سيانيد الذهب (-RS-Au-CN) المميزين، وقد إشتملت الدراسة ايضاً على حساب العمر الأيوني التقريبي لمعقد ثيولات سيانيد الذهب.

وتم الحصول أيضاعلى معقد الذهب مع مركب كبتوبرل (captopril) (أحد الثيولات) في حالة بللورية. ووجد أن هذا المركب يكون مبلمر عالي الكثافة عند إذابته في المحلول المائي. وقد أستخدم هذا المعقد في دراسة تفاعلات التبادل مع الثيومالات وأيون السيانيد في المحاليل المائية وذلك بإستخدام الرنين النووي المغناطيسي لعنصر الكربون-١٣. ووجد أن إرتباط ذرة الذهب بأيون السيانيد أقوى من إرتباطه بالثيومالات. وأمكن ملاحظة المتشكلين الجانبي والقطري (cis-trans) لمعقد الذهب مع كبتوبرل على خطوط الطيف للرنين النووي المغناطيسي للكربون-١٣.

و أشتمل البحث أيضاً على دراسة التفاعل المصحوب بتكسرمعقدات الذهب المرتبطة بمتصل ثلاثي الكل الفوسفين وأيون السيانيد المميزلعنصرالنيتروجين-١٥، (-R3PAuCN) حيث أن R تعني ميثيل-إيثيل-فينل-أيزوبروبل، بواسطةالرنين النووي المغناطيسي لعنصرالفوسفور-٣١ وعنصرالنيتروجين-١٥. ووجد أن المركبات الناتجةمن هذا التكسر في المحاليل المائية هما ثنائي سيانيد الذهب(-Au(CN)2) وثنائي (ثلاثي الكل فوسفين)الذهب(١) (+Au(PR3)2). ولوحظ أيضاً أن خط الطيف للرنين النووي المغناطيسي لعنصرالفوسفور-٣١ يعطي قمتين على الرغم من إختلاف مجموعة الالكل (R=Me,Et,ph,i-Pr)، بينما خط الطيف للرنين النووي المغناطيسي لعنصر النيتروجين-١٥ يعطي قمة واحدة فقط .

CHAPTER ONE

INTRODUCTION

Tobacco smoke contains over 3000 chemicals, of which only relatively few have been investigated regarding their pharmacological and toxicological effects on the body (1). Cigarette smoke contains hydrogen cyanide (HCN) in concentration of about 0.5 μg/ml (2).

It is well known that the gold(I) thiolate drugs (polymer) do not enter red blood cells (3,4). But the polymeric gold complexes react with the cyanide ion to yield the aurocyanide complex ion, $Au(CN)_2^-$, which is readily taken up by red blood cells (5-10). Thus, chrysotherapy patients who are tobacco smokers accumulate gold in their red blood cells from injectable drugs, while nonsmokers do not (11). Cyanide is probably acting as a shuttle to carry gold into red blood cells, and it is unlikely that the aurocyanide complex ion is bound within the cell. So cyanide from the inhaled smoke alters the metabolism of gold, therefore the reaction of cyanide with gold(I) thiolates in vivo are therapeutically significant (8).

It was found that thiolate complexes react with cyanide (CN^-) even at the low concentration forming an intermediate, RS-Au-CN^-, which disproportionates to give $Au(CN)_2^-$ that enters red blood cells and changes the metabolism of gold drugs (5,7).

Objectives

The main objectives in this research are as follows:

1. To study the interaction of the labelled cyanide $C^{15}N^-$ ion with gold(I)thiomalate and gold(I)thioglucose.
2. Synthesis of a new gold(I)captopril complex as a 1:1 ratio of gold:captopril. This complex was prepared in a crystalline form.
3. To study the exchange reactions of gold(I)captopril with thiomalate and cyanide ion using ^{13}C NMR spectroscopy.
4. Preparation of some R_3PAuCl complexes [where PR_3 = PEt_3, PPh_3, $P(n\text{-Propyl})_3$ and P(MeEtPh)].
5. Preparation of $R_3PAuC^{15}N$ where PR_3 = PMe_3, PEt_3, PPh_3, and $P(i\text{-Pr})_3$.
6. ^{15}N NMR studies in methanolic solution of $R_3PAuC^{15}N$ complexes, and interpretation of the spectral results with respect to their equilibrium constants.

CHAPTER TWO

LITERATURE REVIEW

Gold, the first pure metal known to man, has been valued since the very earliest times and even today has a special interest connected with its value as a metal. Gold is the 79th element in the Periodic Table. It has a single s electron outside a complete d shell with an electronic configuration of:

$$1s^2\ 2s^2\ 2p^6\ 3s^2\ 3d^{10}\ 4s^2\ 4d^{10}\ 4f^{14}\ 5s^2\ 5p^6\ 5d^{10}\ 6s^1.$$

1. Oxidation States Of Gold

Compounds of gold having the oxidation states -I, 0, I, II, III and V have been characterized and reported (12), with I and III being the most common. Very few examples of Au(-I) are known, CsAu and RbAu, which are ionic crystals containing auride ions (13,14).

Au(I) ($5d^{10}$) has a closed d shell and a pronounced tendency toward covalent rather than ionic metal-ligand bonds is apparent. Indeed it forms stronger complexes with the more polarizable

anions.

The thermodynamic stability of AuL_2 complex depends on type of ligand L attached to the gold atom (15).

For anionic ligand the trend is as follows:

$$CNO^- < CNS^- \sim Cl^- < Br^- < I^- << CN^-.$$

For neutral ligand the trend is as follows:

$$Ph_3PO < Me_2S < Py < AsPh_3 < NH_3 < C_6H_{11}NH_2 << PPh_3.$$

The most stable being complexes containing π-acid ligands i.e. cyanide and phosphine.

Gold(I) complexes have large variety of different ligands. Gold(I) halides, have long been known and their structures have been characterized. Early interest in compounds of sulfur and gold also was shown. Examples of ligands containing sulfur bonded to gold(I) are thiolates, sulfides, thioethers and thioureas. Gold(I) forms stable coordination compounds with phosphorus, mainly with triorganophosphine ligands, with a general formula:

$$R_3P\text{-}Au\text{-}X \quad \text{and} \quad (R_3P\text{-}Au\text{-}PR_3)^+X^-.$$

where X is a halide ion (16).

Higher oxidation states contain unfilled d orbital, i.e. Au(II)($5d^9$) (16,17), and Au(v)($5d^6$) (18), although known, are

extremely unstable.

Au(III) has been synthesized with various ligands. Gold forms trihalides with fluorine, chlorine, and bromine (16). The large majority gold-halides complexes have the general formula AuX_4^-. Such haloaurate complexes, and especially the tetrachloroaurate complex, are components of numerous salt-like compounds. Gold trihalides known to form stable complexes with many ligands such as nitriles, amines, phosphine oxides, sulfides, and triorganophosphines (16).

2. Structure And Bonding In Au(I)

Au(I) adopts a coordination number of 2, 3, or 4 in solid state and in solution as shown in Table 1.

The coordination number of two is very common, the coordination number of three may be common in solution as indicated by the ease of ligand exchange on Au(I), and the coordination number of four including Au-Au bond may be more common than presently recognized. (Figure 1 shows complexes having coordination number of two).

TABLE 1 Some Variations of Au(I) Coordination Number (15).

Example	gold coordination number	geometry
$Au(CN)_2^-$	2	linear
AuCN	2	linear (polymeric)
$AuCl(PCl_3)$	2	linear
$AuCl(PPh_3)_2$	3	trigonal planar
$Au(CN)_2(o\text{-phen})^-$	4	square planar
$Au(ditertiaryphosphine)_2^+$	4	tetrahedral
Linear Au(I) complexes with Au-Au bonds	4	square planar

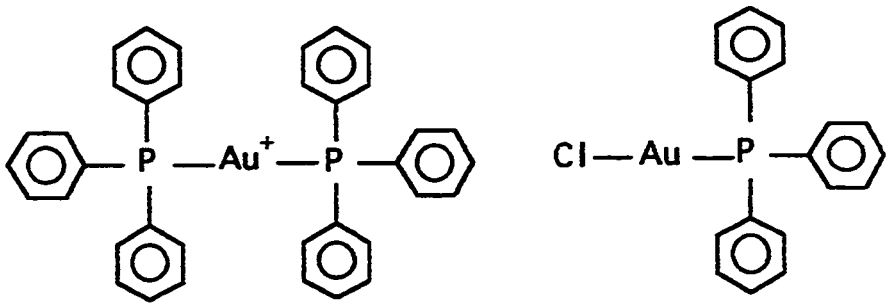

bis(triphenyl phosphine)gold(I)

chloro(triphenyl phosphine)gold(I)

Figure 1 Examples of two coordinate gold(I) complexes.

Other examples which provide linear 2-fold coordination are AuCN polymer and AuCl which form chains with bidentate cyanide (15), or bridging Cl ligands (16):

-Au-C-N-Au-C-N-Au-

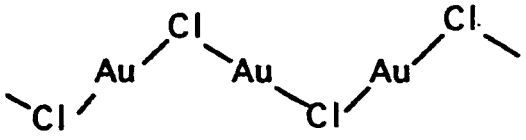

Two different bonding schemes have been proposed for gold(I) complexes depending on the type of ligand attached and the way of bonding. The simpler explanation supposes donation from the ligands to the empty 6s and $6p_z$ orbital of the gold atom (the z axis being the

ligand-gold-ligand axis). An alternative explanation, involving the formation of two sd_{z^2} hybrid orbitals (one empty, one occupied), supposes the occupied hybrid to lie in the xy plane, and donation to take place into the empty hybrid directed along the Z-axis. In both models π acceptance can take place from the d_{xz} and d_{yz} orbitals (19).

Three and four-coordinated gold(I) complexes with phosphine ligands have been characterized. In the solid state tris(triphenylphosphine)gold(I) cation and chlorobis(triphenylphosphine)gold(I) are planar three-coordinate complexes (20,21), as shown in Figure 2.

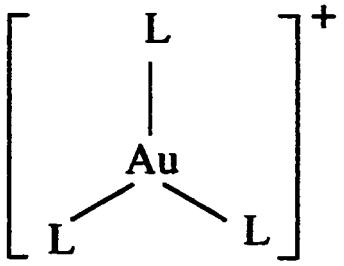

Figure 2 General structure of three-coordinate gold(I) complexes.

Four coordinate complexes with phosphine ligands have been prepared and analyzed by elemental analysis and spectroscopic methods. From the spectroscopic data they are assumed to be

tetrahedral in accordance with expectation (22,23).

The formation of tris and tetrakis (thiolate) complexes is less likely, a possible reason is because of the large charge buildup which would make the $[(RS)_3Au]^{2-}$ and $[(RS)_4Au]^{3-}$ ions energetically less favourable. Even in the absence of overall charge effects of gold, the formation of a 3-coordinate gold(I) requires the formation of sp^2 hybrid, which entails an additional energetic requirement for involvement of a second 6p orbital on gold. Thus the combination of charge buildup and hybridization effects will render discrete three and four-coordinate gold(I) thiolates much less stable than the corresponding phosphine complexes, which maintain a positive charge (12).

3. Structure And Bonding In Au(III)

Gold(III) generally forms square-planar four-coordinate complexes which are typical of d^8 metal ions of the second and third row transition elements. Typical complexes which have been characterized crystallographically (24,25) include $AuCl_4^-$, and Ph_3PAuCl_3 are shown in Figure 3.

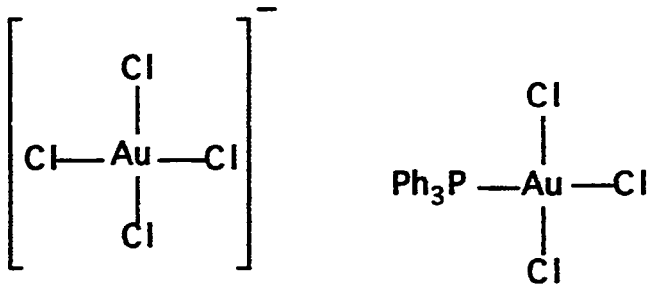

Figure 3 Typical mononuclear square planar gold(III) complexes.

The tendency to form four-coordinate complexes with gold(III) is sufficiently strong that complexes of empirical formula AuL_3, such as $AuBr_3$ and $AuCl_3$, in fact, contain bridging groups to complete the four-coordination about the gold and are correctly formulated as Au_2Br_6 (26) and Au_2Cl_6 (27) as shown in Figure 4.

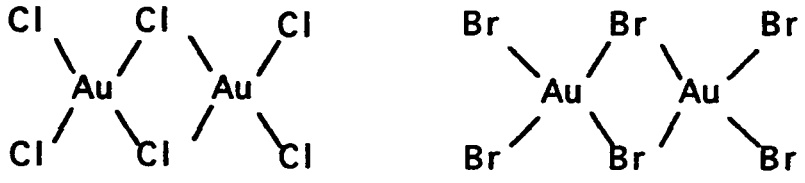

Figure 4 Four-coordinate gold(III) complexes with bridging ligands.

Five and six coordinate complexes have been prepared including trans-diiodobis(o-phenylene-bis(dimethylarsine)gold(III)

(28), [ClAu(tetraphenylporphyrin)] (29), and Br_3Au(2,9-dimethyl-phenanthrene) (30).

4. An Early Start Of Gold Drugs

The biological use of gold can be traced back as far as the Chinese in 2500 B.C. (15). The element is one of the easiest to obtain in pure form, and up to the eighth century metallic gold was considered to be the cure-all for every known disease. Chemical knowledge was advancing, and by the thirteenth century auric chloride was recommended for the treatment of leprosy. Even in the eighteenth and nineteenth centuries gold compounds were popular drugs for every disease, often producing favourable results (15).

Koch's experiments on the effect of AuCN on bacterial growth in 1890 represent the beginning of gold molecular pharmacology and attempts to design gold drugs (15). AuCN was lethal to tubercle bacilli in the test tube. However, it was much less effective when introduced into the blood serum of infected animals. Attempts to put this discovery to clinical use met with partial success for skin tuberculosis and syphilis, but toxic side reactions were severe. The period of 1913-1927 was a time of intense search for Au(I) compounds of lower toxicity. At this stage organic thiols were

introduced as ligands.

Gold caught the public imagination from 1925-1935. These years have been termed the "gold decade" in tuberculosis treatment (15). However laboratory ground work on the curative effect was insecure, and toxicity was still a problem, although the clinical benefits were erratic, there was an astonishing acceptance of the drug during these years, followed by a rapid rejection without the immediate introduction of a substitute.

It was during the gold decade, in 1927 when Au(I) compounds for the treatment of arthritis was introduced (15). It was mistakenly assumed that a relationship existed between chronic polyarthritis and tuberculosis. However, good results were reported and these compounds have remained in clinical use ever since. According to medical opinion now, they are as effective as any other available drug for difficult cases, and are amongst the few drugs that can alter the course of the disease.

Some commonly used drugs are represented in Figure 5 with their trade names and abbreviations (31).

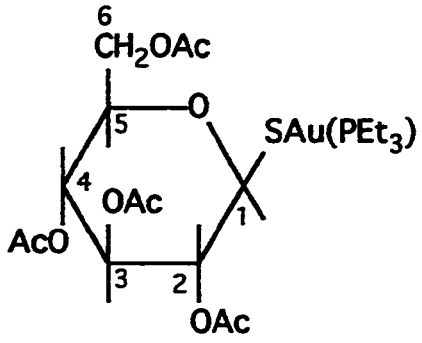

Auranofin
(AF)

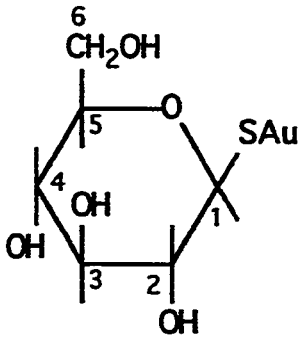

gold thioglucose
(Solganal) (Autg)

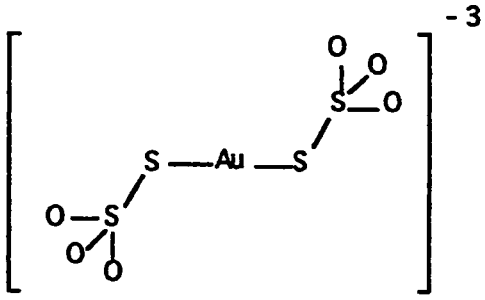

gold sodium thiosulfate
Sanochrysin

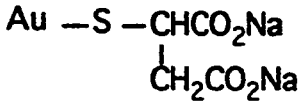

gold sodium thiomalate
(Myochrysin) (Autm)

$Cl\text{-}Au\text{-}P(CH_2CH_3)_3$

chloro(triethylphosphine)gold(I)

Figure 5 Structures of some important gold drugs.

5. The Biological Activity Of Gold Drugs

Gold is an element which is present in the body only in subtrace levels, but which can be accumulated upon environmental exposure or due to deliberate introduction to the organism.

The distribution of gold following injections of its compounds has been thoroughly investigated and it appears to be widely dispersed throughout the body. In a systematic study using rats, soluble compounds such as gold(I)thiomalate, gold(I)thioglucose and gold thiosulfate were found to concentrate in the liver, spleen and kidney with the greatest concentration in the kidney (32,33). These compounds were eliminated primarily via urinary excretion. Insoluble compounds, such as colloidal gold and gold sulfide, accumulate in the same organs, but with the greatest concentration in the liver and with fecal excretion as the primary route of elimination. Also, a much larger percentage of the gold remained localized at the site of the injections. The concentration of gold in the liver, kidneys and spleen following injection of various gold compounds has also been observed with rabbits, mice, and humans (34,35).

The natural accumulation of gold in the blood is known to be small. Its concentration is below 1 ng/g tissue (36,37). During gold

chemotherapy this value increases dramatically.

Numerous investigations have found that gold in the blood stream is localized mostly in the plasma fraction of humans (38,39), rabbits (40) and rats (32).

Because the primary pathogenesis of rheumatoid arthritis is in the joints and particularly the synovia, the delicate lining lubricating the joints which is disrupted during rheumatoid arthritis, the physiology and to a lesser extent biochemistry of gold in the joints during rheumatoid arthritis has been investigated. Gold accumulates in the joints, with greater concentration in inflamed joints than in those which are unaffected (38,41-46).

6. Gold(I)Thiomalate

Gold thiolate complexes are widely used in the treatment of rheumatoid arthritis (15,47,48). The most widely used gold complex, Myochrysin or sodium gold(I)thiomalate (Autm; disodium salt of gold(I)mercaptobutanedioic acid) is a 1:1 complex of gold to sodium thiomalate. The structure (31) of this complex is shown in Figure 6.

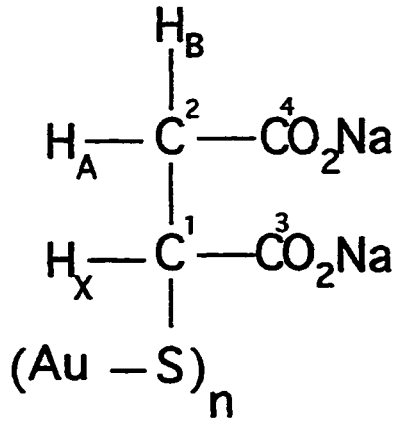

Figure 6 Structure of Autm.

Sodium gold(I)thiomalate can be prepared by mixing thiomalic acid (RSH) and Au(III) in aqueous solution at a 3:1 ratio (49). Reduction occurs as some of the ligands are oxidized and the others stabilize the Au(I). In its simplest form the equation would be:

$$3\ RSH + AuCl_4^- \Longrightarrow Au(I)SR + RS\text{-}SR + 3\ HCl + Cl^- \qquad \text{(eq. 1)}$$

Gold(I) shows a strong preference for linear coordination in most of its complexes. The structures of gold(I)thiomalate could have three possible structures: linear, dimer or boat (50). These structures are represented in Figure 7. Lowering pH, or increasing concentration or increasing the ionic strength of the solution of Autm, generally will increase the polymerization and change the structure of Autm, which in effect will increase the broadening of ^1H and ^{13}C NMR peaks and change their chemical shifts (50).

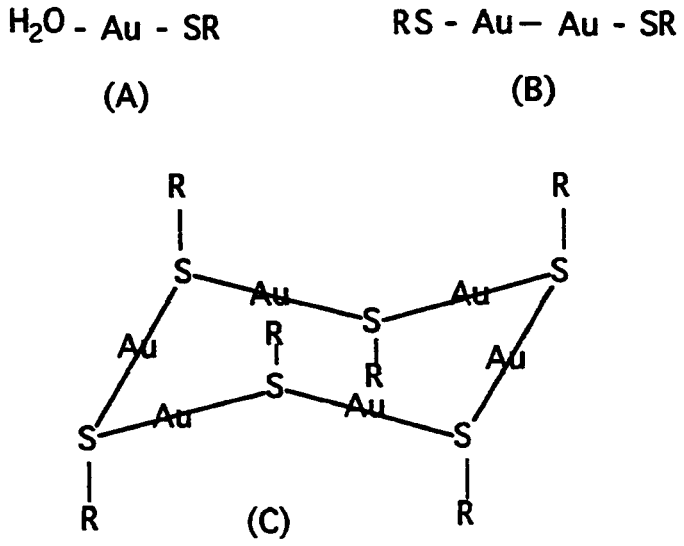

Figure 7 The possibilities of gold(I)thiomalate structures in aqueous solution.

A variety of thiols can react with gold(I)thiomalate in aqueous solution as shown in the following equations:

$$1/n\ (Autm)n + RSH \rightleftharpoons tm\text{-}Au\text{-}SR + H^{+} \qquad \text{(eq. 2)}$$

$$RSH + tm\text{-}Au\text{-}SR \rightleftharpoons RS\text{-}Au\text{-}SR + tmH \qquad \text{(eq. 3)}$$

where both equations have been observed, and equation 3 occurs upon the presence of excess thiol (51).

^{1}H and ^{13}C NMR spectroscopy was used to examine the in vitro interaction of Au(I)tm with thiomalic acid (52-54), glutathione (52,53), L-cysteine derivatives (52,54), D-penicillamine (52), and ergothionine (55). It is found that at a 1:2 mole ratio of Autm:thiol, thiomalate (Htm) is ejected as a free ligand. The rates and activation parameters for thiol-exchange reactions of some of these species have been reported (52).

The ^{1}H NMR spectrum of Autm is shown in Figure 8 together with the changes produced by the addition of cyanide and thiomalate. The addition of 0.4 molar equivalents of cyanide produced considerable broadening and loss of fine structure of all peaks. It is likely that this is due to exchange reactions involving thiomalate

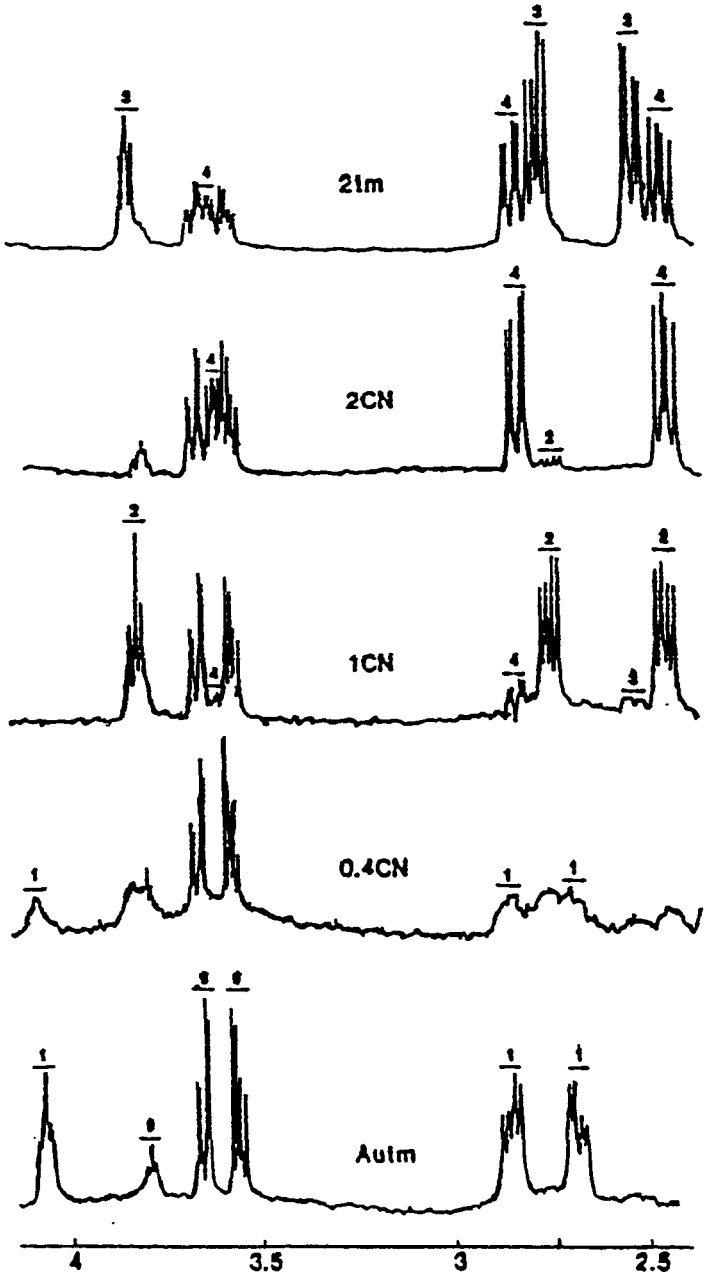

Figure 8 ^{1}H NMR spectra of 2 mM Autm in absence and presence of 0.4, 1, and 2 molar equivalents of cyanide and 2 molar equivalents of thiomalate.

Key: resonances from Autm (1), tm-Au-CN^- (2), $Au(tm)_2^-$ (3), free thiomalate (4) and glycerol (g).

that are of intermediate rate on the NMR time scale, or to the formation of high molecular weight polymeric species. The addition of one equivalent of cyanide to Autm produced a complex spectrum in which all thiomalate peaks were sharper than they were for Autm. The major species showed an ABX spectrum present as a quartet. These resonances are probably due to a mixed complex, tm-Au-CN^-. Minor peaks were also present at a ratio of cyanide:Autm at a 1:1 ratio. Resonances corresponding to a small proportion of free thiomalate were clearly present. The addition of a further equivalent of cyanide (to have Autm:CN^- at 1:2 ratio) again produced changes in the ^1H NMR spectrum with the resonances of the major peaks being identical to those of free thiomalate. Resonances corresponding to a small proportion of the intermediate mixed complex were also present (5).

The release of thiomalate is consistent with the production of $[Au(CN)_2]^-$ (5):

$$\text{Autm} + \text{HCN} \overset{k_1}{\rightleftharpoons} [\text{tm-Au-CN}]^- + \text{H}^+ \qquad \text{(eq. 4)}$$

$$[\text{tm-Au-CN}]^- + \text{HCN} \overset{k_2}{\rightleftharpoons} [\text{Au(CN)}_2]^- + \text{Htm} \qquad \text{(eq. 5)}$$

Chemical shifts and coupling constants of ^1H NMR resonances of gold(I)thiomalate and free thiomalate are given in Table 2.

TABLE 2 Chemical Shifts and Coupling Constants of ^1H NMR Resonances of Gold-Thiomalate Complexes and Free Thiomalate (5).

	Chemical Shifts δ (ppm)			Coupling constants J (Hz)		
	CH_x	CH_A	CH_B	J_{AB}	J_{AX}	J_{BX}
Autm	4.074	2.854	2.683	15.8	7.8	6.6
Thiomalate	3.611	2.827	2.446	15.3	5.7	9.7
$[Autm_2]^-$	3.828	2.760	2.517	15.6	8.8	6.3
$[tm\text{-}Au\text{-}CN]^-$	3.821	2.741	2.439	15.4	7.4	7.6

Recorded at pH* 7.4; ^1H chemical shifts are relative to sodium 3-(trimethylsilyl)-1-propanesulphonate as an internal standard.

Chemical shifts in the ^{1}H NMR spectrum of $Au(tm)_2^-$ were close to those of the presumed mixed complex, tm-Au-CN^-. This is consistent with similarities in their electron distributions and chemical structures. In both cases, each thiomalate is bonded to only one gold atom. By contrast, the sulfur bridging in Autm leads to a deshielding and the greatest chemical shifts of resonances was due to the proton of the CH group attached directly to sulfur.

^{13}C NMR studies of reactions between ^{13}C-enriched cyanide and Au(I)tm produced further evidence of the formation of the mixed ligand complex, $[tm\text{-}Au\text{-}CN]^-$, and finally the production of $[Au(CN)_2]^-$ (5). At different ratios of ^{13}C-cyanide:Autm, two peaks were clearly present in the ^{13}C NMR spectra as shown in Figure 9. The mixed gold(I)thiomalate cyanide species gave rise to a broadened peak at low cyanide:Autm ratios which sharpened and shifted downfield as further cyanide was added. This may due to an equilibrium exchange reactions.

The resonance attributed to $[Au(^{13}CN)_2]^-$ had a chemical shift of 154.27 ppm at cyanide to Autm ratios between 0.4 and 1.5. This corresponds to previously reported chemical shift of 154.2 ppm

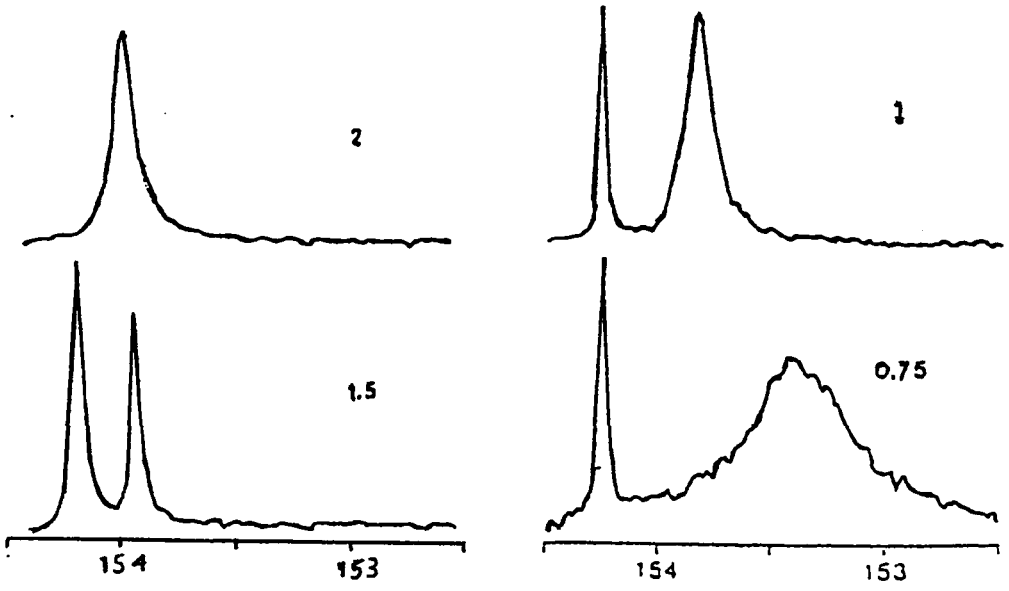

Figure 9 ^{13}C NMR spectra of solutions containing different molar ratios of ^{13}C-cyanide:Autm. downfield resonance is due to $[Au(CN)_2]^-$ and upfield resonance to $[tm\text{-}Au\text{-}CN]^-$.

for $[Au(^{13}CN)_2]^-$ (56). Within the cyanide to Autm range of 0.4-1.5, the linewidth at half height ($\Delta\upsilon_{1/2}$) varied, reaching a minimum of 3.3 Hz at a ratio of 1. At a ratio of cyanide to Autm of 2:1, the $\Delta\upsilon_{1/2}$ of the $[Au(^{13}CN)_2]^-$ peak increased to 12.7 Hz with a slight upfield shift to 154.05 ppm. The addition of a third equivalent of cyanide produced a further marked broadening of the $[Au(^{13}CN)_2]^-$ peak together with a further upfield shift to approximately 148 ppm. These changes in the $\Delta\upsilon_{1/2}$ and chemical shift are consistent with a chemical exchange reaction occurring between bound and free cyanide (chemical shift 114.5 ppm) at an intermediate rate on the NMR time scale (ca.4000 s^{-1}) (5). Chemical shifts of ^{13}C NMR resonances of gold(I)thiomalate complexes and free thiomalate are given in Table 3.

TABLE 3 Chemical Shifts δ (ppm) of ^{13}C NMR Resonances of Gold(I)-Thiomalate Complexes and Free Thiomalate.

compound	C_1	C_2	C_3	C_4
Autm	182.10	47.57	47.90	179.54
Thiomalate	181.67	42.38	45.61	180.45
$[Au(tm)_2]^-$	185.20	43.40	47.90	181.40
$[tm\text{-}Au\text{-}CN]^-$	184.30	43.47	47.96	180.52

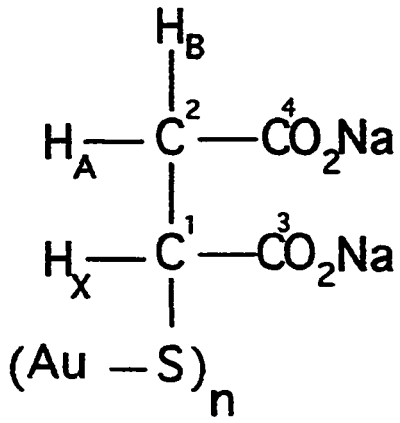

Structure of Autm.

7. Gold(I)Thioglucose

Gold(I)thioglucose have been used to treat rheumatoid arthritis for many years, but less than gold(I)thiomalate (15). Gold(I)thioglucose (Autg, Solganal) is a 1:1 complex of gold to thioglucose. The structure (31) of gold(I)thioglucose is shown in Figure 10.

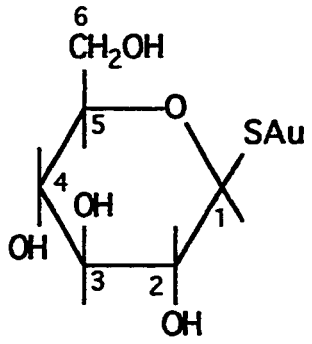

Figure 10 Structure of gold(I)thioglucose.

Gold(I)thioglucose was synthesized by addition of Natg to the aqueous solution of $NaAuCl_4$. The assumed reaction (57,58) is:

$$Au^{3+} + 3\ tg^{-} \Longrightarrow Autg + tg\text{-}tg + 3\ HCl + Cl^{-} \qquad \text{(eq. 6)}$$

Other method for preparing gold(I)thioglucose was proposed by the

reaction of AuX_2^- generated in situ with thioglucose (12).

$$AuCl_4^- + SO_{2(gas)} \Longrightarrow AuCl_2^- \qquad \text{(eq. 7)}$$

$$AuCl_2^- + tg^- \Longrightarrow Autg + Cl^- \qquad \text{(eq. 8)}$$

Unlike glucose, which exists as an equilibrium mixture of the α and β conformers and exhibits resonances arising from each conformer (59,60), thioglucose exists only as the β-form and has only six signals in the ^{13}C NMR spectrum (61).

The ^{13}C NMR spectrum of gold(I)thioglucose, Autg, is presented in Figure 11. Six intense peaks corresponding to the peaks of thioglucose are present along with five weaker peaks for impurity which is proposed to be as the sulfinic acid derivative of thioglucose, tgO_2H (61). However, they are broadened considerably due to the polymerization of the compound in solution. The chemical shifts of α-glucose (α-glu), β-glucose (β-glu), β-D-thioglucose (Htg) and gold(I)thioglucose (Autg) are presented in Table 4.

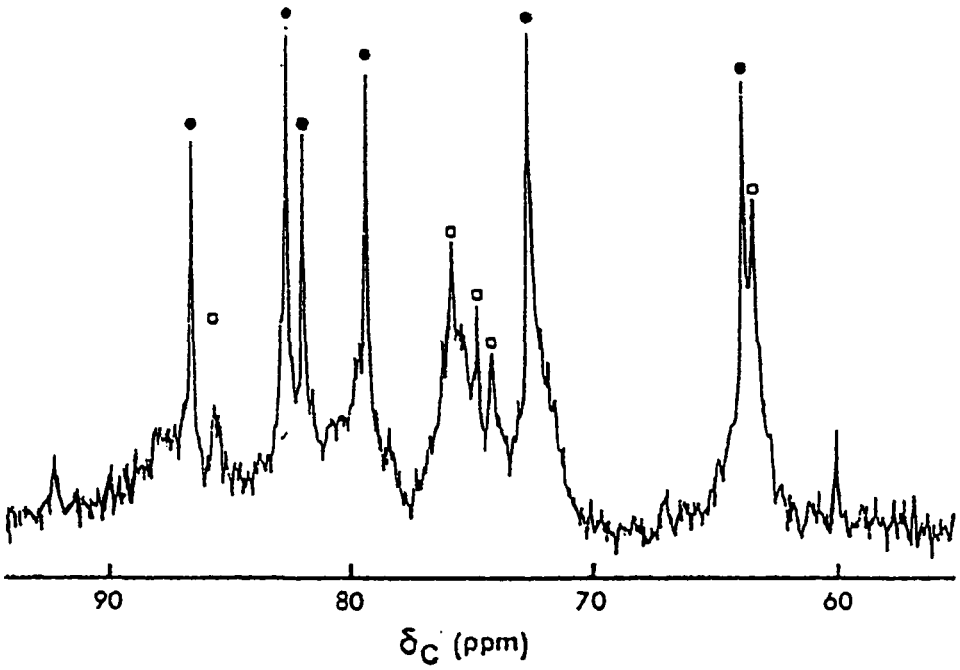

Figure 11 ^{13}C NMR spectrum of gold(I)thioglucose at pH* 7.4. • = Htg, ▫ = impurity.

TABLE 4 ^{13}C NMR Chemical Shifts of Glucose, Thioglucose and Gold(I)thioglucose (61).

compound	C_1	C_2	C_3	C_4	C_5	C_6
β-glucose	96.70	74.90	76.70	70.40	76.50	61.60
α-glucose	92.80	72.30	73.60	70.40	72.30	61.60
Htg	86.52	79.64	82.48	73.06	81.04	63.99
Autg	86.80	79.57	82.88	72.77	82.25	63.66
tgO_2H	95.99	74.74	85.59	74.02	75.95	63.50

The reaction between unlabelled and labelled $^{13}CN^-$ with gold(I)thioglucose have been studied using ^{13}C NMR spectroscopy (7). As shown in Figure 12A the Autg ^{13}C NMR spectrum is very broad. When 1 equivalent of CN^- (unlabelled) was added to the Autg solution the broad peaks of Autg became sharper. Also, a small peak at 153.31 ppm due to $Au(CN)_2^-$ appeared. In solution as the concentration of CN^- was increased relative to Autg (Figure 12 B and C) no significant change was observed in the high field region. This shows that the different species of tg^- exist in fast exchange and

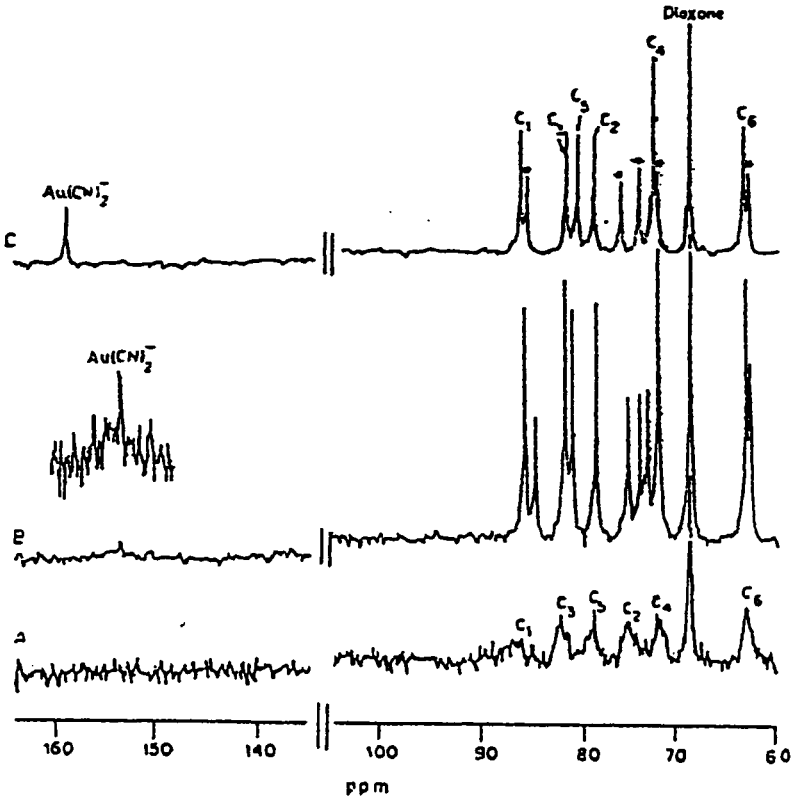

Figure 12 The noise-decoupled ^{13}C NMR spectra of 0.15 M Autg:CN^- (unlabelled) at different molar ratios: (A) 1:0, (B) 1:1, and (C) 1:4.

only averaged resonances of tg^- are observed.

The equilibrium reactions are proposed to exist:

$$Autg + HCN \rightleftharpoons tg\text{-}Au\text{-}CN^- + H^+ \qquad \text{(eq. 9)}$$

$$tg\text{-}Au\text{-}CN^- + HCN \rightleftharpoons Au(CN)_2^- + Htg \qquad \text{(eq. 10)}$$

$$Autg + Htg \rightleftharpoons Au(tg)_2^- + H^+ \qquad \text{(eq. 11)}$$

$$2\ (tg\text{-}Au\text{-}CN)^- \rightleftharpoons Au(CN)_2^- + Au(tg)_2^- \qquad \text{(eq. 12)}$$

The ^{13}C NMR chemical shifts of Autg and the addition of CN^- at different ratios are summarized in Table 5.

TABLE 5 ^{13}C NMR Chemical Shifts of Gold(I)Thioglucose:CN^- at Various Molar Equivalent Ratios (7).

Gold(I):tg:CN^-	C_1	C_2	C_3	C_4	C_5	C_6
1 : 1 : 0	85.75	74.01	80.89	70.82	77.61	61.74
1 : 1 : 1	84.89	77.61	80.81	70.88	80.11	62.01
1 : 1 : 2	84.88	77.71	80.63	71.10	79.63	62.05
1 : 1 : 4	85.04	77.73	80.50	71.26	79.45	62.13

When ^{13}C-enriched cyanide was added to Autg solution (7), two more resonances appeared in the low field region (Figure 13). The down-field resonance, which is due to $Au(^{13}CN)_2^-$ is less intense and appeared at 154.36 ppm. The more intense peak is due to tg-Au-$^{13}CN^-$ and appeared at 153.17 ppm. As the concentrations of $^{13}CN^-$ were increased the tg-Au-$^{13}CN^-$ and $Au(^{13}CN)_2^-$ resonances merged, as shown in Figure 13 C to E.

Equation 12 indicates that the linear RS-Au-CN^- complex is unstable in solution and tends to give $Au(SR)_2^-$ and $Au(CN)_2^-$.

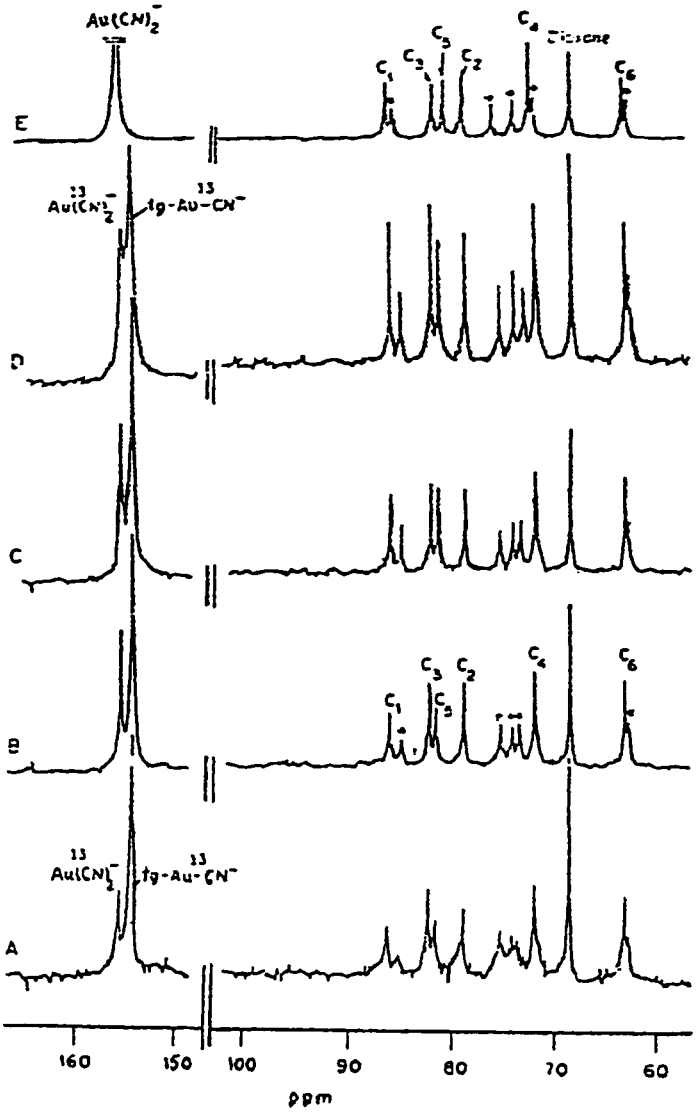

Figure 13 The 50 MHz ^{1}H noise-decoupled ^{13}C NMR spectra of 0.15 M Autg:$^{13}CN^-$ (labelled) at different molar ratios: (A) 1:0.25, (B) 1:0.5, (C) 1:0.75, (D) 1:1, and (E) 1:2.

8. Gold(I)Captopril

It has been known for many years that the venoms from several species of snake have an effect on blood pressure, in most cases reducing it. In the late 1960's, researchers were successful in fractionating the vasodilating components of the venom of the South American snake, Bothrops Jararaca (62). The most active component was a nonapeptide, teprotide, which proved to be very effective in the treatment of hypertension for humans (63).

In the process of determining which fragments of the nonapeptide were important for activity, and trying out many modifications eventually led to the development of captopril (cap); 1-[2(S)-3-mercapto-2-methyl-1-oxopropyl]-L-proline.

Economically producing captopril is viable. As a drug captopril is orally active, and is an effective hypertensive agent, reducing blood pressure in many patients whose hypertension could not be controlled by other available drugs (64-67). More recently captopril has been used with some success to treat rheumatoid arthritis (68).

It is well-known that proline-containing peptides (Figure 14) normally exist as an equilibrium mixture of *trans* and *cis* isomers with respect to the peptide bond involving the proline amino group (69).

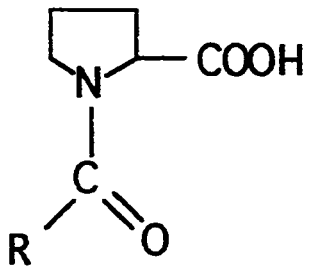

Figure 14 Proline structure.

Thus, captopril is expected to be present in aqueous solution as the *trans* and *cis* forms Figure 15, I and II, respectively, with the relative population of the two forms dependent on the protonation state of the molecule (69-71).

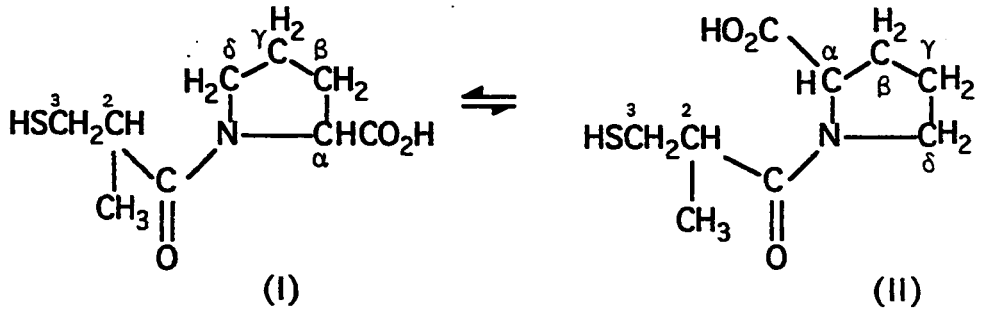

Figure 15 Structures of *trans-cis* isomers of captopril in equilibrium.

Nuclear magnetic resonance (NMR) spectroscopy was used to determine the presence of *trans-cis* isomers of captopril and to study the solution chemistry of the two isomers. The two isomers of captopril can be observed in both acidic and basic solution from pH 1 to pH 13 by both ^{1}H and ^{13}C NMR spectra (72).

The 50.3 MHz ^{13}C NMR spectra for captopril (H_2A) is shown in Figure 16, HA^- and A^{2-} conjugated bases of captopril are also shown. (H_2A is captopril with both acidic protons of carboxylic group and sulfhydryl group, HA^- is captopril with sulfhydryl group only, and A^{2-} is captopril without any acidic proton).

Generally, the *cis* isomer of HA^- and A^{2-} of captopril are less kineticly stable than the *trans* isomer. However, the *cis* isomer is still detectable by NMR spectroscopy. For H_2A, however the *cis* isomer is much less kineticly stable to an extent that it was not easy to detect by NMR. Resonance assignment and chemical shifts of these isomers are given in Table 6.

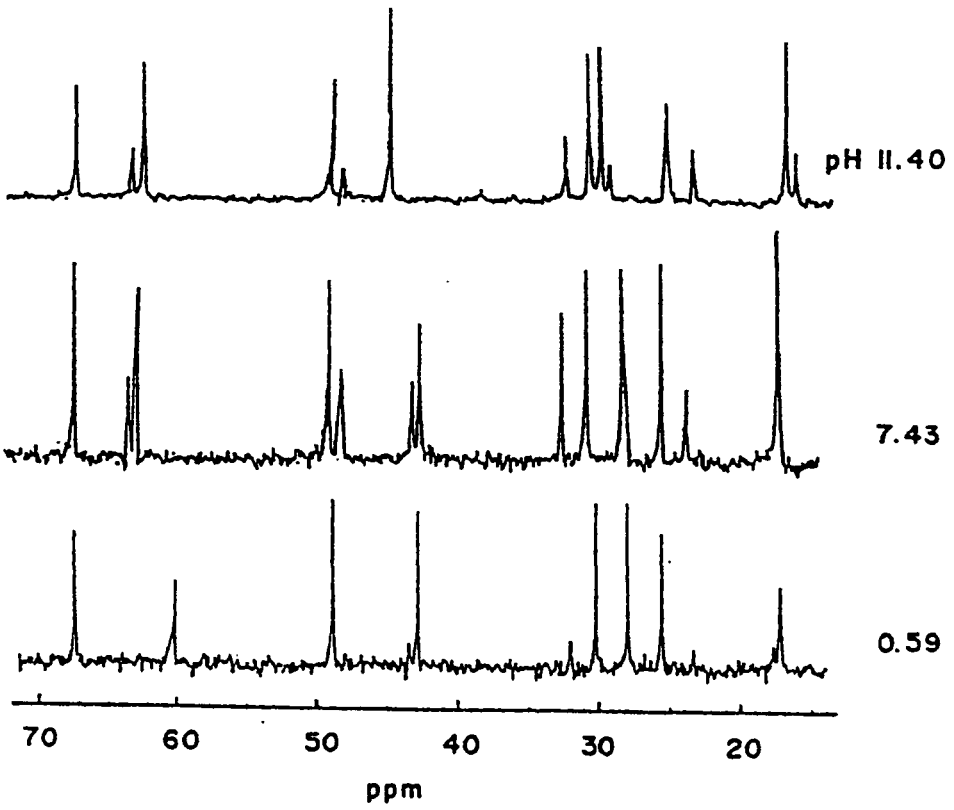

Figure 16 The 50.3 MHz ^{13}C NMR spectrum of 0.55 M captopril as a function of pH in H_2O solution containing 0.16 M NaCl.

TABLE 6 ^{13}C NMR Chemical Shifts for Captopril (72).

		H_2A	HA^-	A^{2-}
C_3	*trans*	27.630	27.730	29.689
	cis	b	27.560	29.101
C_2	*trans*	42.553	42.333	44.832
	cis	43.141	42.850	b
CH_3	*trans*	16.898	16.901	16.751
	cis	b	16.750	16.089
CON	*trans*	177.153	176.505	178.476
	cis	b	177.373	179.726
C_α	*trans*	60.049	62.550	62.475
	cis	b	63.210	63.211
C_β	*trans*	29.836	30.433	30.497
	cis	31.673	32.190	32.261
C_γ	*trans*	25.204	25.130	25.131
	cis	b	23.290	23.293
C_δ	*trans*	48.655	48.800	48.802
	cis	47.722	47.921	47.772
CO_2^-	*trans*	177.006	180.534	178.402
	cis	b	b	179.729

(b) Resonances either too small to detect or not resolved

The more abundant isomer has been suggested to *trans* conformation on the basis of the following (71) :

i) The *trans* isomer is the most abundant for the related proline molecules.

ii) The chemical shift of the amide carbon of the *trans* isomer undergoes a characteristic desheilding upon deprotonation of the carboxylic group, as shown in Figure 17.

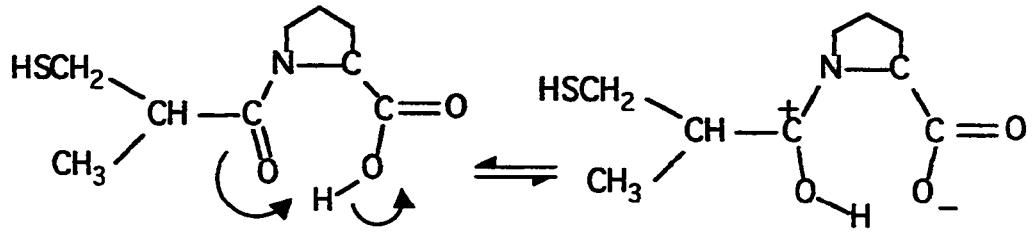

Figure 17 Deprotonation of carboxylic group and desheilding of the amide carbon of the *trans* isomer of captopril.

Acid dissociation constants for the carboxylic acid and sulfhydryl groups of the *trans* and *cis* isomers of captopril were determined using ^{13}C NMR spectroscopy. The average values obtained for pK_1 of the *trans* and *cis* isomers are 3.52 and 2.86 respectively, where K_1 is the acid dissociation constant for the carboxylic acid group (72).

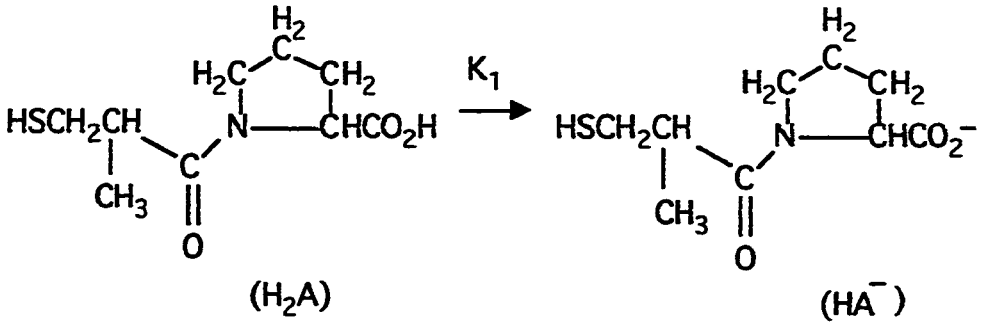

Equation 13 Dissociation of carboxylic acid group of captopril.

Also, the average values for pK_2 were found to be 9.71 and 9.99 for the *trans* and *cis* isomers, respectively, where K_2 is the sulfhydryl dissociation constant (72).

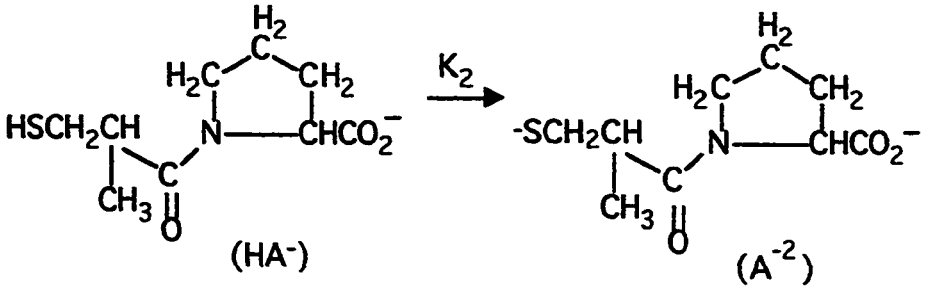

Equation 14 Dissociation of sulfhydryl group of captopril.

The results in Figure 18 indicates that for captopril, the relative stability of the *trans* and *cis* conformations depends markedly on protonation state. The enhanced stability of the *trans*

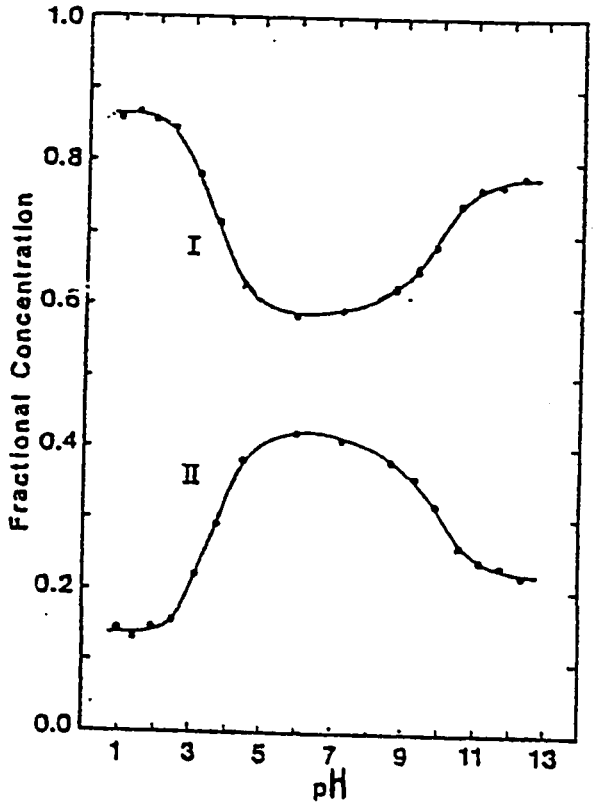

Figure 18 Relative stability of the *trans* and *cis* isomers of captopril depending on protonation state.

conformation of the H_2A form relative to that of the HA^- form is probably due to stabilization of the *trans* form of H_2A through intramolecular hydrogen bonding between the carboxylic acid hydrogen and the amide carbonyl oxygen (70,71,73). Suchs hydrogen bond is not possible in the *cis* isomer, as shown in Figure 19.

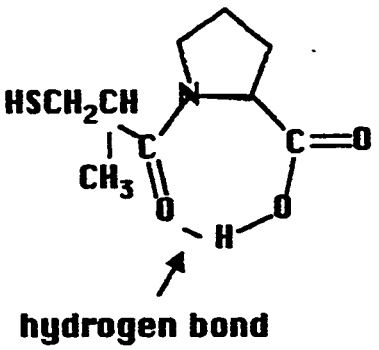

Figure 19 Stabilization of the *trans* form of (H_2A) by hydrogen bonding between carboxylic acid hydrogen and the amide carbon oxygen.

The *trans* isomer stability (70,71) is enhanced by the intramolecular hydrogen bond as observed in other *trans* isomer of the carboxylic acid forms of related small peptides such as, proline as in Figure 19.

Since the hydrogen involved in the proposed hydrogen bond is the one titrated when the *trans* isomer goes from H_2A to

HA^-, the carboxylic acid group of the *trans* isomer would be expected to be somewhat less acidic than that for the *cis* isomer, as is found to be the case (71).

The enhanced stability of the *trans* isomer of the A^{2-} form relative to that of the HA^- form is presumably due to the increased charge-charge repulsion between the deprotonated sulfhydryl and carboxylic acid groups in the *cis* conformation of the A^{2-} form. Space-filling molecular models show the separation of these two groups to be larger in the *trans* conformation (72).

The binding of captopril with zinc(II), cadmium(II), lead(II), and copper(II) has been reported (74,75). Since these studies carried out by potentiometric titrations, the *trans* and the *cis* isomers were not resolved. The interaction of captopril with gold(I) has also been reported (76). The chemical shift differences of the *trans* and *cis* isomers bonded to gold(I) were not resolved because of the overlapping of some resonances. Complexation of $CH_3Hg(II)$ by captopril has also been studied by ^1H and ^{13}C NMR spectroscopy (77).

The equilibrium constants for the *trans(I)* <==> *cis(II)* equilibrium, $K_{eq} = [II]/[I]$, are given in Table 7 for free captopril.

TABLE 7 Equilibrium Constants K_{eq} = [II]/[I] of the *Trans(I)* and *Cis(II)* Isomers of Captopril (77).

pH	Species	K_{eq}
0.59	H_2A	0.17
7.43	HA^-	0.69
12.30	A^{2-}	0.30

A reaction of gold(I)thiomalate Autm with captopril was carried out in aqueous solution at pH* 7.20 using ^{13}C NMR spectroscopy (76). When captopril was added to Autm solution, free thiomalate resonances appeared. As the concentration of captopril was increased to ratios of [Autm]:[captopril] of 1:2 and 1:3 respectively, the free thiomalate resonances increased in intensity, and bound thiomalate resonances almost disappeared at a 1:3 ratio.

The appearance of free thiomalate resonances at a 1:1 ratio indicates that when captopril binds to gold(I), it ejects some of the thiomalate into solution. This shows that captopril may be forming two types of complexes:

the Au(I)-captopril (one ligand per metal) and possibly a thiomalato-gold(I)captopril complex (cap-Au-tm^-)complex (76).

9. Cyanotri(alkyl/aryl)phosphinegold(I) Complexes

Gold(I) as a slightly charged, large, and easily polarizable metal ion which forms particularly stable coordination compounds with phosphorus. Various complexes of this type are known, mainly with triorganophosphine ligands. In the case of the simplest type R_3PAuX numerous examples have been reported. Various R groups are bonded to phosphorus (alkyl-, aryl-, alkylaryl) to form phosphine ligands (16).

Cyanotri(alkyl/aryl)phosphinegold(I) complexes, (R_3PAuCN), have been prepared, isolated and studied. Two methods have been used for preparing R_3PAuCN complexes. The preparation of the R_3PAuCN complexes was carried out by the addition of R_3P to an excess of Au(I)CN in methanol or acetone (R = Methyl (Me), Ethyl (Et), Phenyl (Ph), iso-Propyl (i-Pr), and Cyclohexyl (Cy)). Generally the reaction is almost instantaneous (78). In the other procedure the aqueous solution of potassium cyanide (KCN) was added to the aqueous solution of $[Au(H_2O)(PR_3)]NO_3$ to give R_3PAuCN (79-81). The complex $[Au(H_2O)(PR_3)]NO_3$ has been prepared by the addition of an aqueous solution of silver nitrate, $AgNO_3$, to the ethanolic solution of the R_3PAuCl complex.

The solid-state structures of cyano(triethylphosphine)gold(I)

(80), cyano(trimethylphosphine)gold(I) (81), and cyano(triphenylphosphine)gold(I) (82) have been investigated.

From the crystal structures of these complexes the phosphine and cyanide ligands appear to coordinate to the gold atom forming linear two coordinate complexes. Solid state, Mossbauer (80,83), infrared (79,80,84) and Raman (79) spectroscopies have also been used to provide information about the bonding of cyano group with gold(I) atom in the presence of phosphine ligand.

Recently, the solution chemistry of cyanotri(alkyl/aryl)-phosphinegold(I) complexes has been studied. Ligand scrambling reactions of gold(I) complexes that are initiated by the presence of excess ligands have been known for some time (85-87). Also, the reaction in equation 15 has been studied, such disproportionation takes place without the presence of excess ligand:

$$2\ R_3PAuCN \overset{K_{eq}}{\rightleftharpoons} (R_3P)_2Au^+ + Au(CN)_2^- \qquad \text{(eq. 15)}$$

The ligand scrambling reaction of R_3PAuCN to from $(R_3P)_2Au^+$ and $Au(CN)_2^-$ in solution has been studied for R = Me, Et, Ph, i-Pr and Cy (78). The reactions are conveniently studied by ^{13}C and ^{31}P NMR

and infrared spectroscopy. Since the equilibrium constants (K_{eq}) of these reactions have been affected by extrinsic effect such as initial concentration of the complex $[R_3PAuCN]_o$, ionic strength of the medium and intrinsic factors such as steric hindrance and electronic properties of the phosphine ligands, they were reported at constant concentration. Solvent and ionic strength of the medium are kept constant (78).

The effect of the initial concentration, and the effect of the presence of NH_4NO_3 on the equilibrium constant were studied only for Et_3PAuCN. It was found that as the initial concentration of Et_3PAuCN complex was increased the K_{eq} also increased. There is also a direct relationship between K_{eq} for Et_3PAuCN and the concentration of NH_4NO_3. The K_{eq} of these scrambled reactions have been monitored using ^{13}C and ^{31}P NMR spectroscopy (78).

CHAPTER THREE

EXPERIMENTAL AND RESULTS

1. Chemicals

Gold(I)thiomalate and gold(I)thioglucose were purchased from ICN K and K Labs (Plainview, NY). Captopril was provided by Bristol Myers-Squibb Institute for Medical Research, Princeton, New Jersey. Sodiumtetrachloroauratedihydrate, chloro(trimethylphosphine)-gold(I), chloro(tri-iso-propylphosphine) gold(I), and phosphine ligands [triethylphosphine PEt_3, triphenylphosphine PPh_3, tri-n-propylphosphine $n\text{-}Pr_3P$ and methylethylphenylphosphine P(MeEtPh)] were obtained from Stream Chemical Co. $KC^{15}N$ (99%) and $K^{13}CN$ were purchased from Merck Sharp and Dohme, Canada. Potassium cyanide, thiomalic acid, 99.7% D_2O, 40% NaOD in D_2O, 35% DCl in D_2O, CD_3OD and all other reagents were obtained from Fluka Chemical Co.

2. pH Measurements

All pH measurements were made at 22°C with a Fisher Accumet pH meter, model 620, equipped with Fisher microprobe combination pH electrode. The pH* indicates the actual meter reading for D_2O solutions with no correction for deuterium isotope effect. The pH* was adjusted by DCl or NaOD as necessary.

3. NMR Measurements

3.1. ^{15}N NMR Measurements

The ^{15}N NMR spectra for the interaction of gold(I)thiomalate and gold(I)thioglucose with labelled ^{15}N cyanide ion were obtained by continuous proton decoupling at 20.266 MHz on a XL-200 NMR spectrometer using D_2O solutions.

The T_1 values were not measured. The spectral conditions were: 5.0 s delay time, 32 K data points, spectral width 10,000 Hz, pulse width 5.0 μs (20°), 10 mm multinuclear probe.

The line shape analysis for the observed resonances was carried out using a library package (88).

The ^{15}N NMR spectra for disproportionation reaction of $R_3PAuC^{15}N$ complexes were obtained at 27.24 MHz on a Jeol 270 spectrometer using CD_3OD solutions at the probe temperature of 300 K.

The T_1 values of any resonance were not measured. The spectral conditions were: 5.0 s delay time, 16 K data points, spectral width 20,000 Hz, pulse width 6.0 μs (20°), and 10 mm multinuclear probe. For the ^{15}N NMR spectra approximately 60,000 scans were accumulated.

The chemical shifts for ^{15}N NMR spectra were measured using a sealed external $NH_4{}^{15}NO_3$ as an external reference which has a resonance at 375.11 ppm relative to pure CH_3NO_2 which has a resonance at 380.2 ppm (89).

3.2. ^{13}C NMR Measurements

^{13}C NMR spectra were measured at 50.03 MHz on a Varian XL-200 spectrometer operating in the pulsed Fourier transform mode. The ^{13}C NMR measurements were carried out with coherent off-resonance ^{1}H decoupling or with broad-band ^{1}H decoupling. ^{13}C NMR chemical shifts were measured relative to internal dioxane or glycerol which occurs at 67.40 ppm and 63.33 ppm respectively upfield from $SiMe_4$. All spectra were recorded after 50,000-70,000 scans.

3.3. ^{31}P NMR Measurements

The ^{31}P NMR spectra were obtained at 109.25 MHz on a Jeol 270 spectrometer using CD_3OD solutions at the probe temperature of 300 K. The ^{31}P NMR chemical shifts are measured from external 1% TMP (90).

The T_1 values were not measured. The spectral conditions were: 1.0 s delay time, 65 K data points, spectral width 40,000 Hz, pulse width 12.0 μs (20°), and 10 mm multinuclear probe. For the ^{31}P NMR spectra approximately 10,000 scans were accumulated.

4. Interaction Of Gold(I)Thiomalate With $KC^{15}N$

The yellow 0.20 M gold(I)thiomalate solution was prepared by dissolving 0.093 g (0.20 mmol) of gold(I)thiomalate in 1.0 ml D_2O. As solid, potassium cyanide (^{15}N labelled) was added gradually to the Au(I)tm solution to give different molar equivalent ratios. The pH* of the solution was kept at 7.40 throughout the titration. Spectra of [Autm]:[$C^{15}N^-$] in the following molar ratio: (A) 1:0.5, (B) 1:1, (C) 1:1.5, (D) 1:2 are shown in Figure 20.

When labelled $C^{15}N^-$ was added as a solid to a 0.20 M Autm solution, only one peak at 260 ppm appeared up to a molar equivalent ratio of 2:1 for [Autm]:[CN^-]. This resonance is attributed to tm-Au-$C^{15}N^-$ complex. However at higher concentrations of $C^{15}N^-$, [Autm]:[$C^{15}N^-$], 2:1.5, the resonance at 265 ppm appeared and increased in intensity as the concentration of CN^- was increased, (Figure 20). From previous work reported in the literature (5,7) it can be concluded that, the resonance at 265 ppm is due to $Au(C^{15}N)_2^-$ complex. The chemical shift and the $\Delta\upsilon_{1/2}$ of the resonances are given in Table 8.

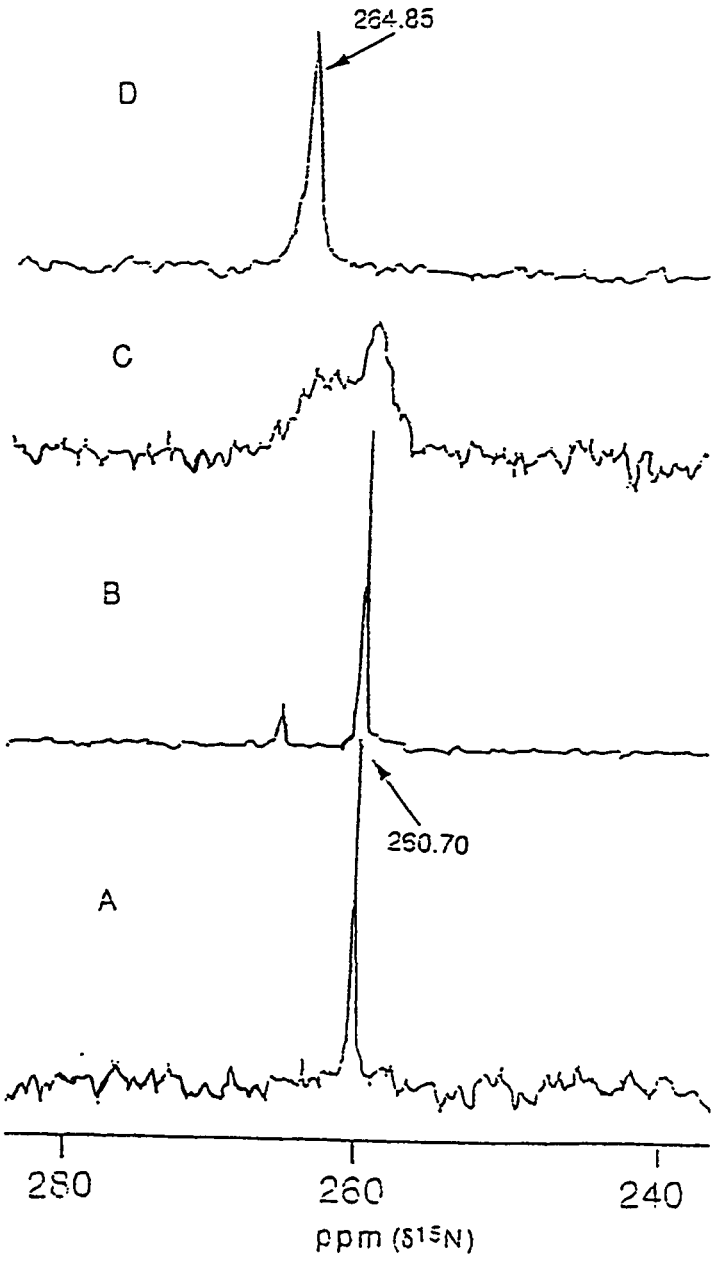

Figure 20 The 20.266 MHz ^{1}H noise-decoupled ^{15}N NMR spectra of 0.20 M Autm:$C^{15}N^{-}$ at different molar ratios: (A) 1:0.5, (B) 1:1, (C) 1:1.5 and (D) 1:2.

TABLE 8 The ^{15}N NMR Chemical Shifts of tm-Au-$C^{15}N^-$ and $Au(C^{15}N)_2^-$ at the Various Concentration Ratios of Autm:$C^{15}N^-$.

[Autm] : [$C^{15}N^-$]	$\delta(^{15}N)$ tm-Au-$C^{15}N^-$	$\delta(^{15}N)$ $Au(CN)_2^-$	Q[a]	$\Delta\upsilon_{1/2}$ (Hz)	τ(s)[b]
0.20 M : 0.050 M	260.61	-	-		
0.20 M : 0.100 M	260.70	-	-		
0.20 M : 0.150 M	260.70	265.94	5.38×10^{-4}	10	0.100
0.20 M : 0.175 M	260.40	265.66	1.42×10^{-2}	10	0.060
0.20 M : 0.200 M	260.24	265.61	3.63×10^{-2}	12	0.045
0.20 M : 0.225 M	260.12	265.70	8.96×10^{-2}	13	0.025
0.20 M : 0.250 M	260.09	265.77	0.124	15	0.020
0.20 M : 0.275 M	260.21	265.57	0.189	40	0.012
0.20 M : 0.300 M	263.26		c	75	0.0028
0.20 M : 0.325 M	263.30		c	55	0.0013
0.20 M : 0.350 M	263.88		c	42	0.0009
0.20 M : 0.400 M	264.85		c	15	-

a = ratio of $[Au(CN)_2^-]^2$ / $[tm\text{-}Au\text{-}C^{15}N^-]^2$

b = life time for tm-Au-CN^- species

c = beyond coalescence

5. Interaction Of Gold(I)Thioglucose With $KC^{15}N$

Gold(I)thioglucose solution of 0.20 M (0.078 g, 0.20 mmol), in 1.0 ml D_2O was prepared. This solution was titrated with the solid $KC^{15}N$, at a pH* 7.4. The Autg solution was yellow during this titration up to the ratio of Autg:$C^{15}N^-$ of 1:0.75. Figure 21 shows the spectra of [Autg]:[$C^{15}N^-$] at different molar ratios as follows: (A) 1:0.25, (B) 1:0.5, (C) 1:0.75, (D) 1:1 and (E) 1:2.

When 0.05 molar equivalent of $C^{15}N^-$ was added as a solid to the 0.20 M Autg solution, two resonances at 260.10 and 265.41 ppm were observed. As the concentration of $C^{15}N^-$ was increased, the resonance at 265.41 ppm increased in intensity up to the ratio of Autg:$C^{15}N^-$ of 1:0.75. However beyond this ratio (e.g. at 1:1) both resonances coalesced and as the concentration of $C^{15}N^-$ was further increased the coalesced resonance became sharper. The chemical shift and the $\Delta\upsilon_{1/2}$ of these resonances are given in Table 9.

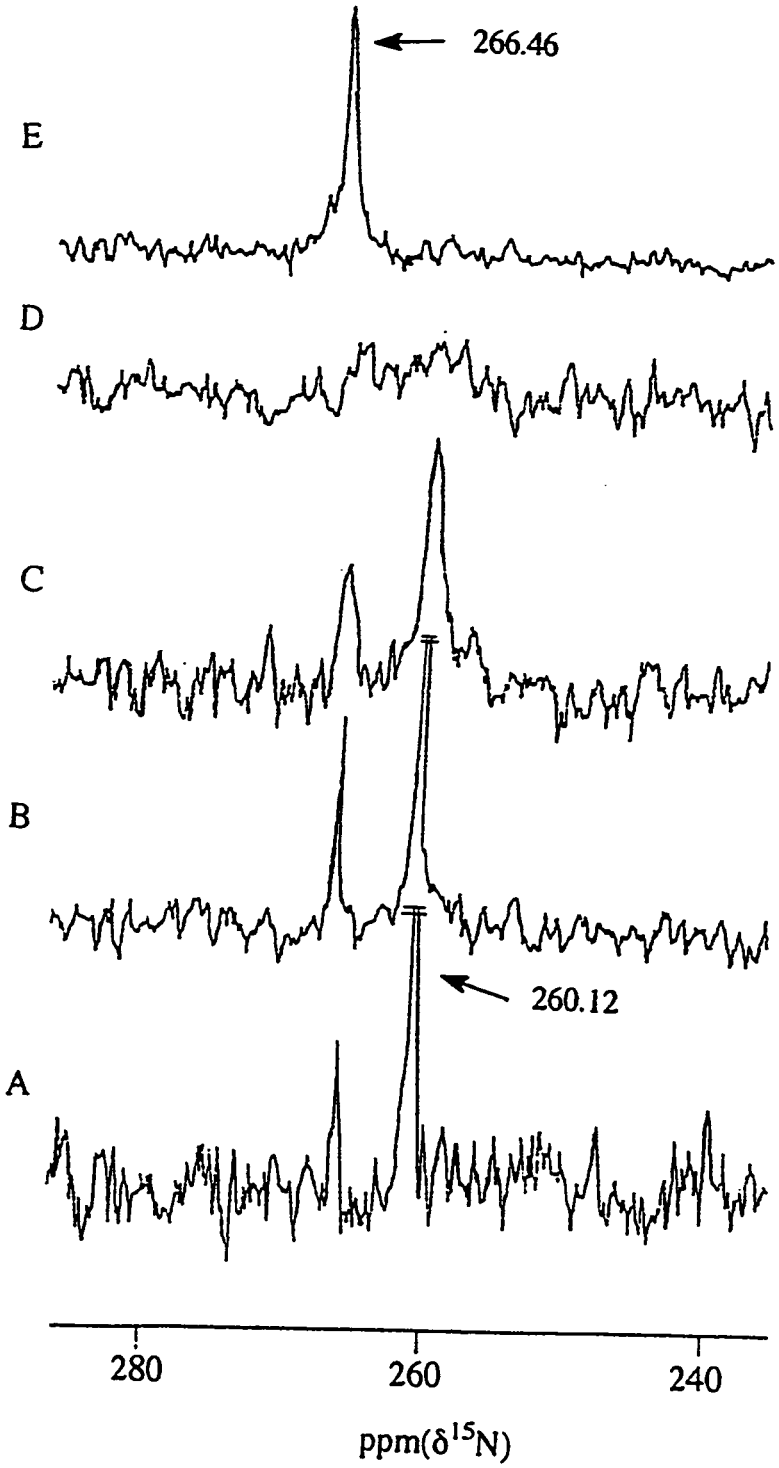

Figure 21 The 20.266 MHz ^{1}H noise-decoupled ^{15}N NMR spectra of 0.20 M Autg:C$^{15}N^{-}$ at different molar ratios: (A) 1:0.25, (B) 1:0.5, (C) 1:0.75, (D) 1:1 and (E) 1:2.

TABLE 9 The ^{15}N NMR Chemical Shifts of tg-Au-$C^{15}N^-$ and $Au(C^{15}N)_2^-$ at the Various Concentration Ratios of Autg:$C^{15}N^-$.

[Autg] : [$C^{15}N^-$]	$\delta(^{15}N)$ tg-Au-$C^{15}N^-$	$\delta(^{15}N)$ $Au(C^{15}N)_2^-$	Q[a]	$\Delta\upsilon_{1/2}$ (Hz)	τ(s)[b]
0.20 M : 0.050 M	260.10	265.41	9.07×10^{-3}	2.2	0.10
0.20 M : 0.100 M	260.30	265.67	1.56×10^{-2}	5.5	0.025
0.20 M : 0.150 M	260.12	265.73	3.08×10^{-2}	28	0.0083
0.20 M : 0.200 M	259.89		c	105	0.0037
0.20 M : 0.300 M	265.65		c	80	0.0020
0.20 M : 0.400 M	266.46		c	16	-

a = ratio of $[Au(CN)_2^-]^2$ / $[tg\text{-}Au\text{-}C^{15}N^-]^2$

b = life time for tg-Au-CN^- species

c = beyond coalescence

6. Gold(I)Captopril Complex

6.1. Preparation Of Gold(I)Captopril Complex

To a solution of chloroauric acid (1.9 g, 5.0 mmol) in deionized water (100 ml) maintained at 0°C, a solution of 2.2'-thiodiethanol (thiodiglycol) (1.2 g, 10.0 mmol) in deionized water (30 ml) was added dropwise with constant stirring. After the mixture became colorless {indicating reduction of Au(III) to Au(I)} (91), a solution of captopril (1.1 g, 5.0 mmol) in deionized water (20 ml) was added. The mixture was stirred for 30 minutes at room temperature. The white precipitate was filtered, washed three times by deionized water, and left to dry overnight (yield 75%, at 241°C- 244°C with decomposition).

6.2. Elemental Analysis

The elemental analysis for hydrogen, carbon, nitrogen and sulfur of gold(I)captopril complex was carried out with Carlo Erba Model 1106 Elemental Analyzer. The analytical data is given in Table 10 along with the calculated values:

TABLE 10 Elemental Analysis of Gold(I)-Captopril Complex.

elements	found%	cal.%
carbon	25.8	26.16
hydrogen	3.5	3.41
nitrogen	3.1	3.39
sulfur	7.4	7.76

6.3. Infrared Absorption Spectra

The infrared absorption spectra in KBr pellets of the pure captopril and Au(I)cap complex were carried out on Nicolet 5D X B FTIR from 4800 to 200 cm^{-1}. The IR spectra of the pure captopril and Au(I)cap complex are shown in Figure 22 and Figure 23 respectively.

The IR spectrum of the Au(I)cap complex shows the disappearance of SH absorption at 2500 cm^{-1} (92). This suggests that gold(I) binds via thiol group of the ligand. Absorption at 345 cm^{-1} was assigned to Au-S resonance (58), however, there was no Au-Cl absorption observed within 310-320 cm^{-1} region (79) which eliminate the possibility of the formation of cap-Au(I)-Cl^- complex.

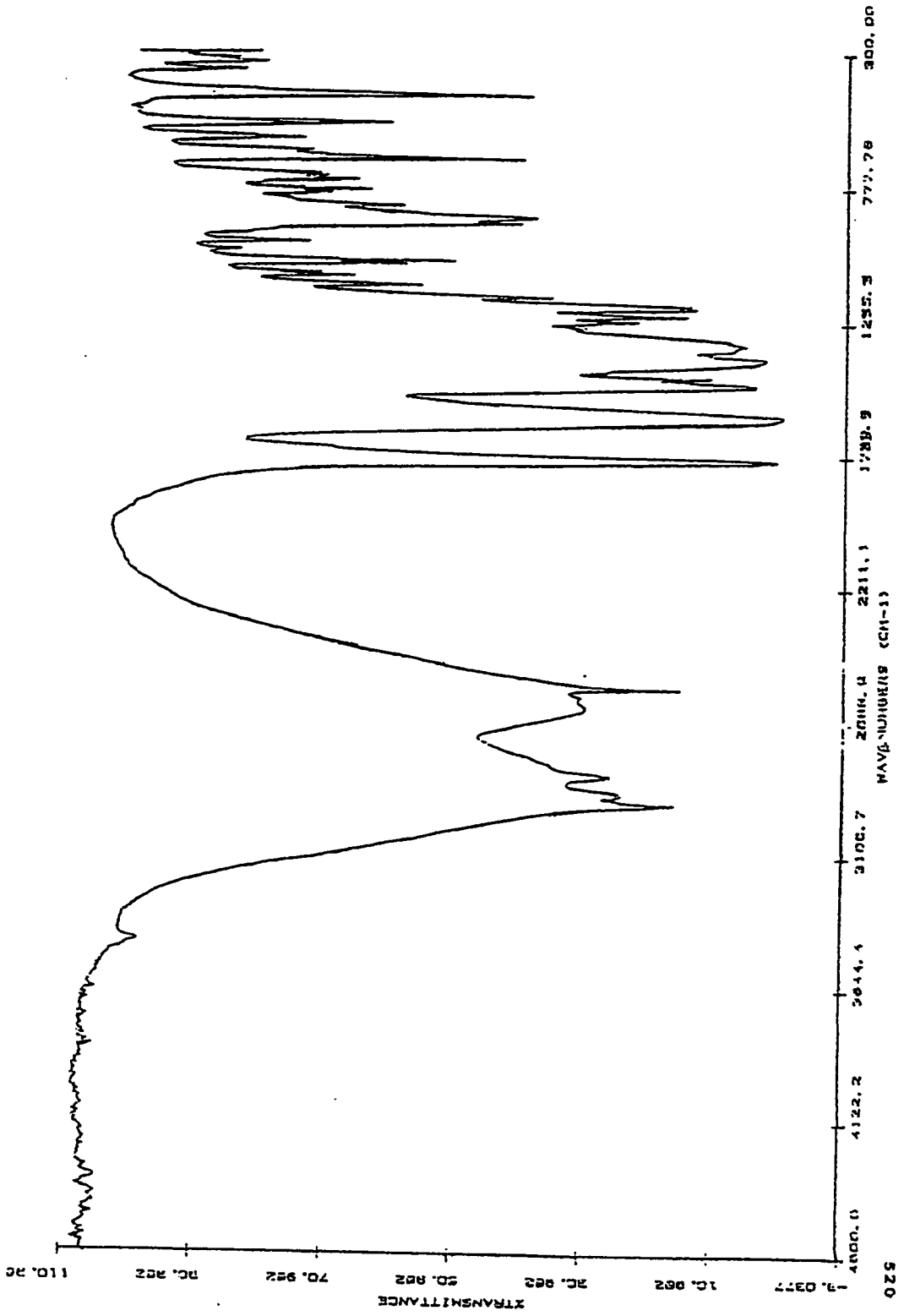

Figure 22 Infrared spectrum of free captopril in KBr pellets.

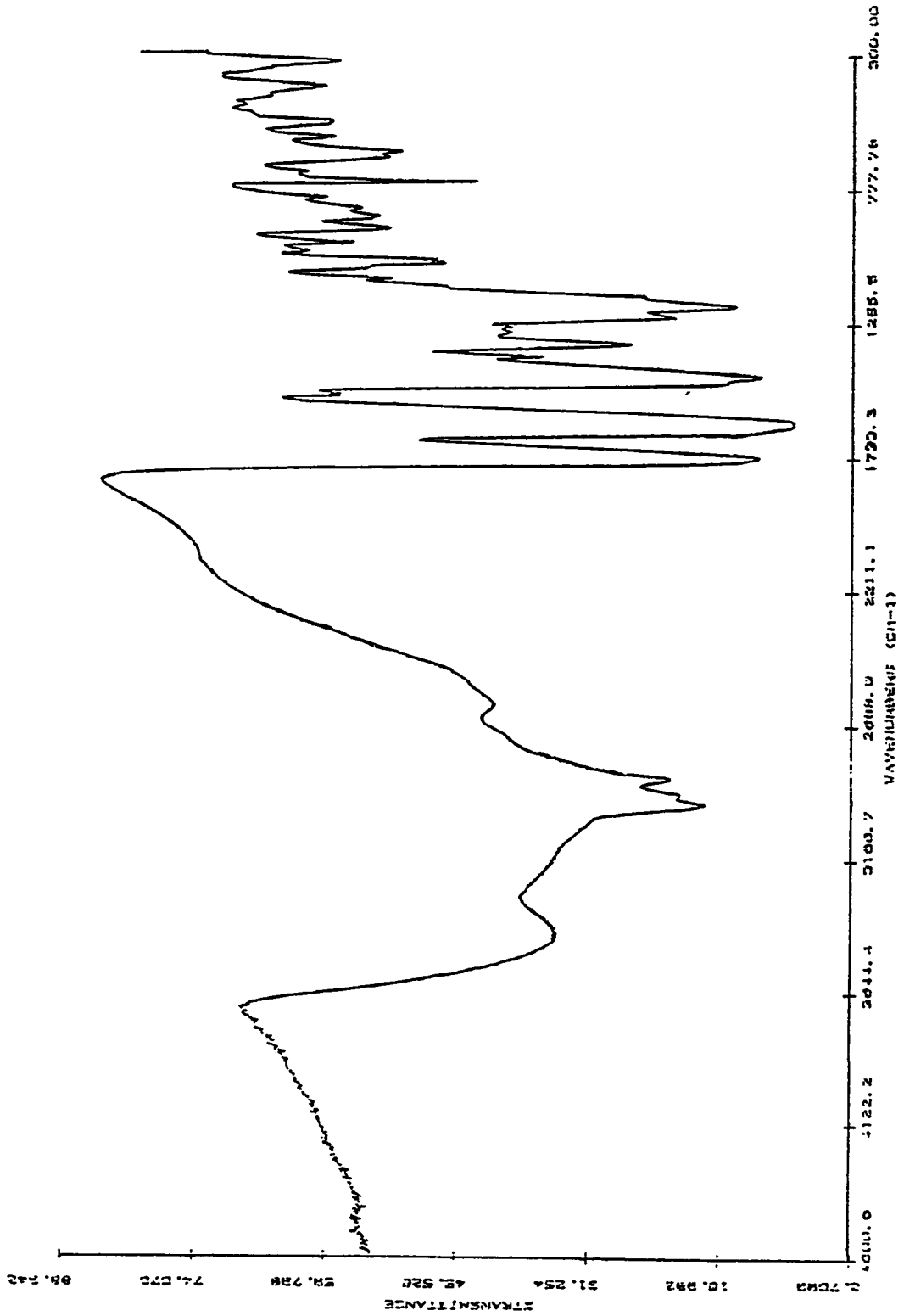

Figure 23 Infrared spectrum of gold(I)captopril complex in KBr pellets.

6.4. Interaction Of Au(I)Captopril With Thiomalate

A solution of Au(I)cap (0.25 M in 2 ml D_2O) was prepared. The Au(I)cap complex is insoluble in water at a pH* lower than 12 and only soluble at high pH*. A concentrated solution of NaOH was used to increase the pH* of the Au(I)cap solution, which was very viscous and colorless. Then ^{13}C NMR spectrum was measured for this solution. It is shown in Figure 24A. This spectrum is very broad.

When one equivalent of solid thiomalate (Htm) (0.25 M) was added to the Au(I)cap aqueous solution, the pH* was decreased and adjusted to the physiological pH* 7.20. Then ^{13}C NMR spectrum was recorded and represented in Figure 24B.

When a second equivalent of solid thiomalate (0.5 M total) was added to the Au(I)cap solution, the pH* again adjusted to 7.20, and the ^{13}C NMR spectrum was recorded and shown in Figure 24C.

From these spectra it can be concluded that when one equivalent of Htm (0.25 M) was added a few captopril resonances appeared as shown in Figure 24B. Also thiomalate bound to gold(I), b_2 = 47.96 ppm and b_1 = 43.57 ppm and free thiomalate resonances f_2 = 45.15 ppm and f_1 = 42.37 ppm appeared in the spectrum.

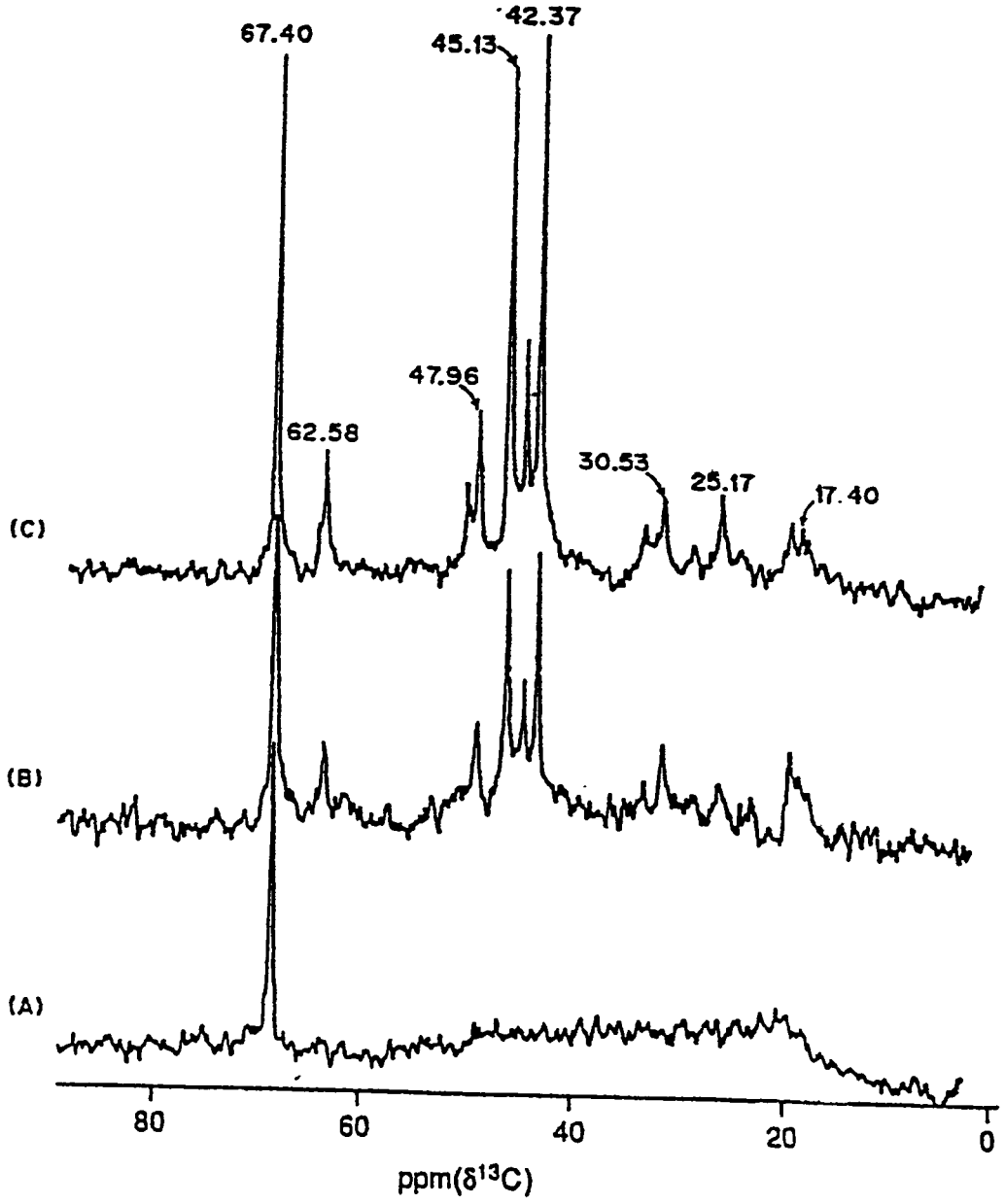

Figure 24 The 50 MHz ^{1}H noise-decoupled ^{13}C NMR spectra of (A) 0.25 M Au(I)cap at pH* 12.20, (B) 0.25 M Au(I)cap:Htm at a 1:1 ratio at pH* 7.20 and (C) 0.25 M Au(I)cap:Htm at a 1:2 ratio at pH* 7.20.

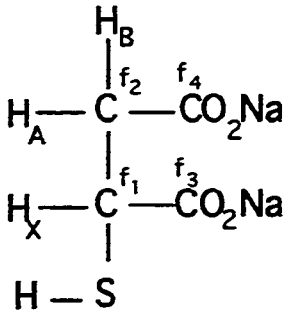

Free thiomalate

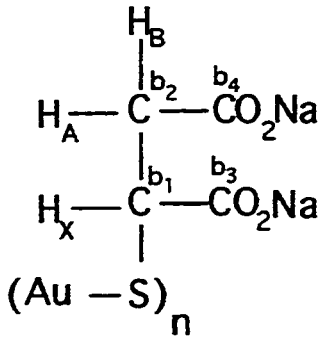

Bound thiomalate

But when a second equivalent of solid thiomalate (0.5 M total) was added to the Au(I)cap solution, the captopril resonances sharpened, a very small enhancement of b_2 and b_1 resonances were observed, and the f_2 and f_1 resonances increased in intensities. These free and bound thiomalate resonances show that it is in equilibrium with Au(I)cap solution. The chemical shifts of various Au(I)cap resonances are given in Table 11.

TABLE 11 ^{13}C NMR Chemical Shifts of Au(I)Captopril and Thiomalate at pH* 7.2.

Resonance Assignments		Free Captopril and free Htm	Au(I):Captopril: Htm 1:1:2
C_3	*trans*	27.72	b
	cis	27.56	b
C_2	*trans*	42.33	b
	cis	42.85	b
CH_3	*trans*	16.90	18.45, 17.40, 16.84
	cis	16.75	-
CON	*trans*	176.51	-
	cis	177.37	-
C_α	*trans*	62.55	62.58
	cis	63.21	63.17
C_β	*trans*	30.43	30.53
	cis	32.19	32.23
$C\gamma$	*trans*	25.13	25.17
	cis	23.29	b
$C\delta$	*trans*	48.80	49.50
	cis	47.92	b
CO_2^-	*trans*	180.53	-
	cis	b	-
b_2	Au-tm	-	47.96
b_1	Au-tm	-	43.57
f_2	Htm	45.13	45.13
f_1	Htm	42.37	42.37

(b) Resonances are either too small to detect or overlapped with other resonances.

6.5. Interaction Of Au(I)Captopril With CN^-

A solution of Au(I)cap (0.25 M in 2.0 ml D_2O) at pH* 12.20 was prepared. ^{13}C NMR spectrum was measured for this solution and shown in Figure 25A.

When one equivalent of KCN as a solid was added to the Au(I)cap solution, it became less viscous, and ^{13}C NMR spectrum was measured at pH* 12.20. The captopril resonances appeared relatively broad.

When another equivalent of KCN was added, the spectrum was recorded at pH*12.20, as it is shown in Figure 25B, the captopril resonances became sharper. The 153.67 ppm and 154.20 ppm resonances were assigned to cap-Au-CN^- and $Au(CN)_2^-$ complexes.

The spectrum of the solution of Au(I)cap and KCN at a molar ratio of 1:2 was recorded again but the pH* was adjusted to 7.20. As shown in Figure 25C, the resonances were assigned for cap-Au-CN^- and $Au(CN)_2^-$ complexes at pH* 12.20 shifted to 154.09 ppm and 155.38 ppm at pH* 7.2.

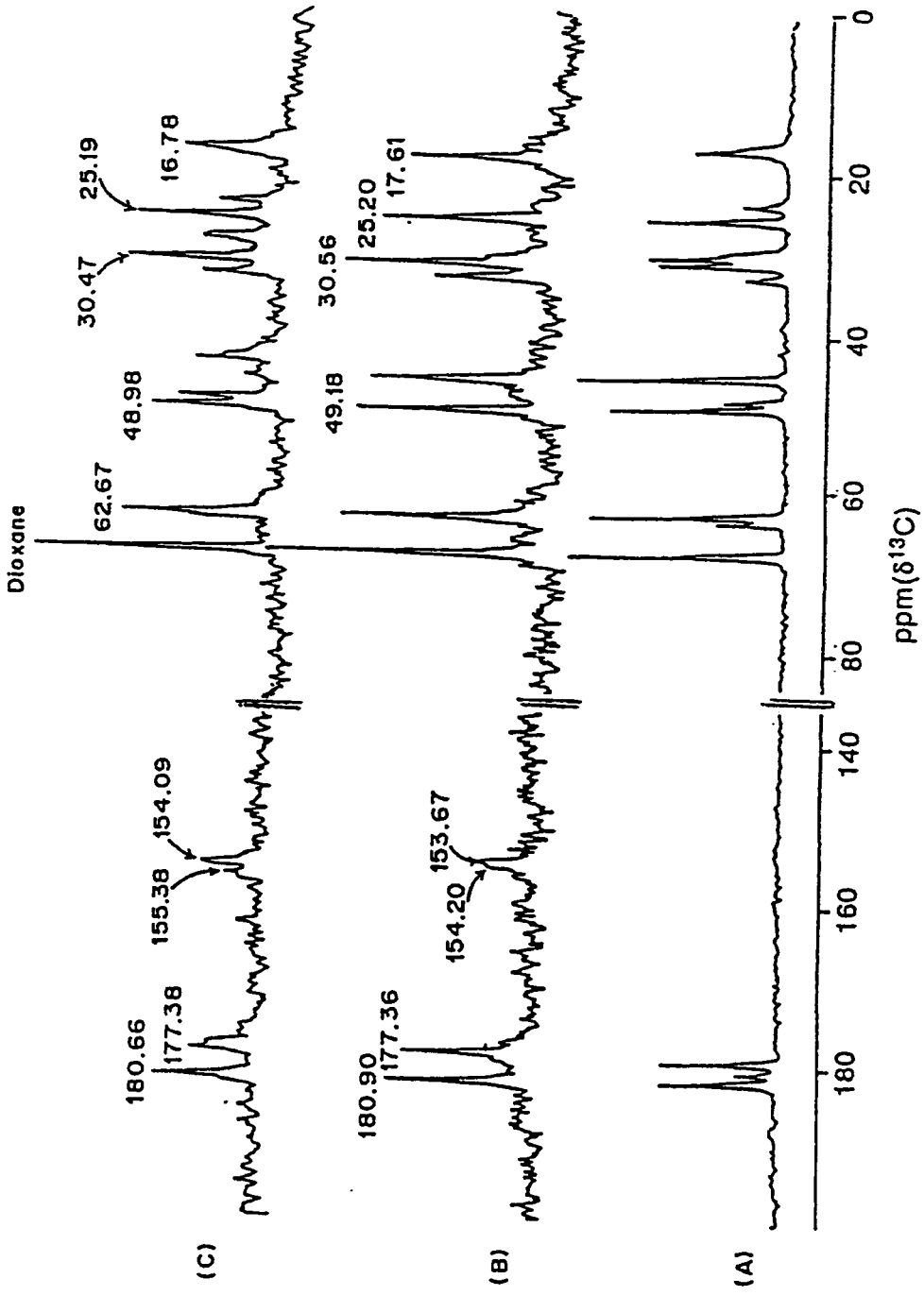

Figure 25 The 50 MHz ^{1}H noise-decoupled ^{13}C NMR spectra of (A) 0.25 M captopril itself at pH* 12.20, (B) 0.25 M Au(I)cap:CN^- at a 1:2 ratio at pH* 12.20, (C) same as (B) but the pH* is 7.20.

The chemical shifts of Au(I)cap in the presence of CN^- are given in Table 12. These assignments are based on similar studies for the reaction of CN^- with Autm and gold(I)glutathione (5,8).

TABLE 12 ^{13}C NMR Chemical Shifts of Au(I)Captopril and CN^- Complexes at pH* 12.20 and 7.20.

Resonance Assignments		Free Captopril at pH* 12.20	Au(I)cap:CN^- (1:2) at pH* 12.20	Free captopril at pH* 7.20	Au(I)cap:CN^- (1:2) at pH* 7.20
C_3	*trans*	29.69	30.56	27.72	27.84
	cis	29.10	29.82	27.56	b
C_2	*trans*	44.83	45.15	42.33	42.39
	cis	b	b	42.85	42.92
CH_3	*trans*	16.75	17.61	16.90	16.78
	cis	16.09	16.28	16.75	b
CON	*trans*	178.50	177.36	176.51	176.80
	cis	179.26	b	177.37	177.38
$C\alpha$	*trans*	62.48	62.75	62.55	62.67
	cis	63.21	b	63.21	63.21
$C\beta$	*trans*	30.50	30.56	30.43	30.47
	cis	32.26	32.38	32.19	32.19
$C\gamma$	*trans*	25.13	25.20	25.13	25.19
	cis	23.29	b	23.29	23.33
$C\delta$	*trans*	48.80	49.18	48.80	48.98
	cis	47.77	b	47.92	47.91
CO_2^-	*trans*	181.06	180.90	180.53	180.66
	cis	180.92	b	b	b
$Au(CN)_2^-$		-	154.20	-	155.38
Cap-Au-CN^-		-	153.67	-	154.09

(b) Resonances are either too small to detect or overlapped with other resonances.

6.6. Interaction Of Au(I)Captopril With Labelled $^{13}CN^-$

A solution of 0.50 M of Au(I)cap was prepared by adding 0.20 g (0.50 mmol) of solid Au(I)cap to 1.0 ml of D_2O then enough NaOH was added to dissolve it. Glycerol was added as a reference. The pH* of the solution was measured to be 13.08. The solution was very viscous and colorless. The spectrum of this solution is shown in Figure 26A.

When 0.125 molar equivalent of (100% labelled) $K^{13}CN$ was added as a solid to the Au(I)cap solution the viscosity decreased and the solution remained colorless. The pH* of the solution was adjusted to 7.4. Then ^{13}C NMR spectrum was recorded, which is shown in Figure 26B. The resonances were broad in the high field region. However, three intense resonances appeared in the low field region. These three resonances were assigned based on the mole ratio of *cis* and *trans* isomers of captopril as cap(c)$Au^{13}CN^-$, cap(t)$Au^{13}CN^-$ and $Au(^{13}CN)_2^-$ at 143.83 ppm, 152.18 ppm and 154.06 ppm respectively (72).

Assuming the T_1 are about the same, the percentage were estimated by measuring the integration of ^{13}C NMR resonances as 36% $Au(^{13}CN)_2^-$, 52% *trans* and 12% for the *cis* complex.

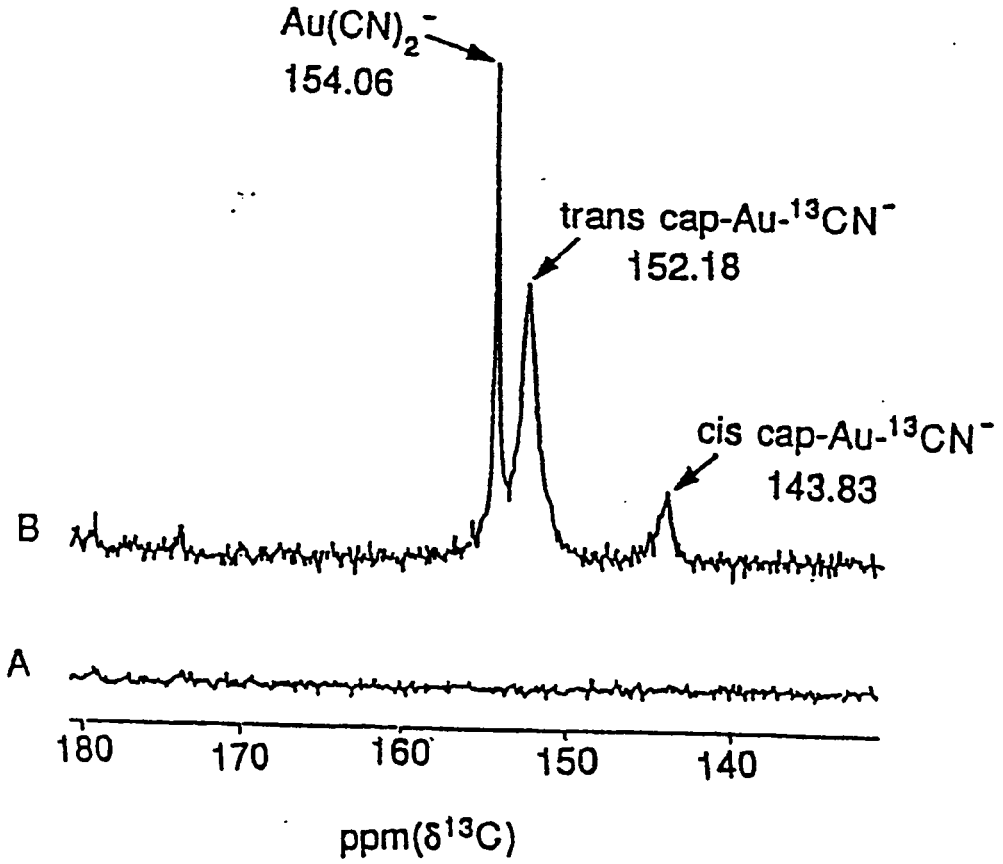

Figure 26 The 50 MHz ^{1}H noise-decoupled ^{13}C NMR spectra of the low field region: (A) 0.50 M Au(I)cap itself at pH* 13.08, and (B) 0.125 M 100% labelled $^{13}CN^-$ added to Au(I)cap solution at pH* 7.40.

6.7. Interaction Of Au(I)Captopril With KCN (10% Label)

A solution of 0.50 M of Au(I)cap was prepared by adding 0.20 g (0.50 mmol) of Au(I)cap to 1.0 ml of D_2O then enough NaOH was added to dissolve it. Glycerol was added as a reference. The solution was very viscous, colorless, and has pH* 13.08.

To the Au(I)cap solution which was previously prepared (10% label) KCN was added gradually, as shown in Table 13. When KCN was added the viscosity of the Au(I)cap solution decreased and the pH* was adjusted for each step. Then ^{13}C NMR spectra were monitored as shown in Figure 27.

TABLE 13 Additions of (10% label) KCN to Au(I)cap Solution with its Measured pH*.

spectrum#	[Au(I)cap]:[KCN] mole ratio	pH*
A	8 : 0	13.08
B	8 : 1	7.35
C	8 : 3	7.50
D	8 : 4	7.50
E	8 : 8	7.60

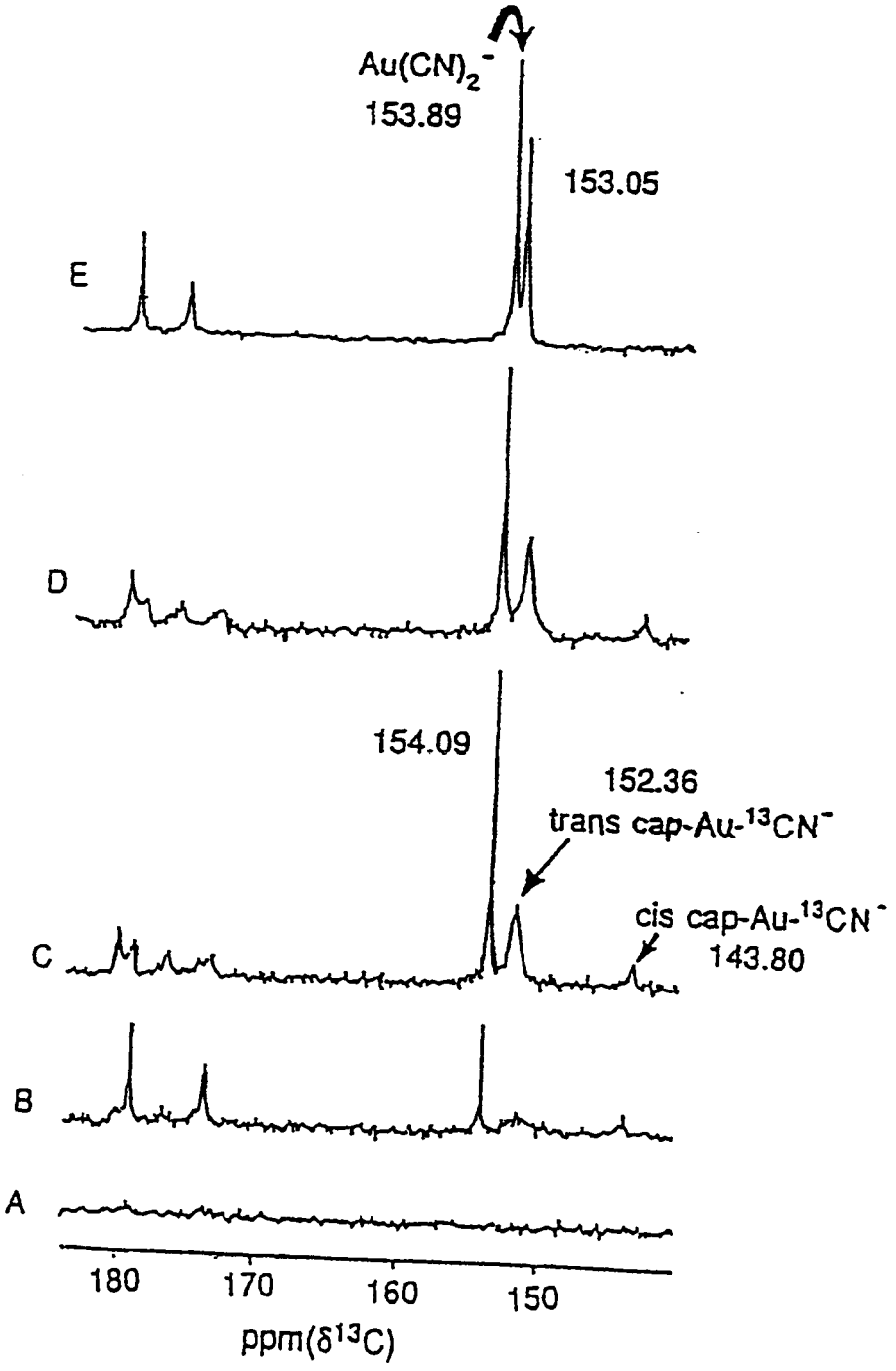

Figure 27 The 50 MHz ^{1}H noise-decoupled ^{13}C NMR spectra in the low field region of (a) 0.50 M Au(I)cap at pH* 13.08, (b)-(e) show the effect of the addition of 10% labelled $^{13}CN^-$ and 90% unlabelled CN^- to 0.50 M Au(I)cap at different molar ratio, as shown in Table 13.

When $K^{13}CN$ (100% label) was added to Au(I)cap solution the three resonances in the low field region appeared for cap(c)$Au^{13}CN^-$, cap(t)$Au^{13}CN^-$, and $Au(^{13}CN)_2^-$. The peaks were very intense compare to other captopril resonances. Because of this the whole experiment was repeated by gradual addition of 10% labelled $^{13}CN^-$ and 90% unlabelled CN^- to the 0.50 M Au(I)cap solution. As shown in Figure 27 B-E (only the low field region is shown), the $Au(CN)_2^-$ resonance at 154.09 ppm was sharp and increased in intensity. Also, as expected, as the concentration of $^{13}CN^-$ was increased the intensity of *trans* and *cis* cap-Au-$^{13}CN^-$ resonances increased. At a 1:1 ratio of Au(I)cap:$^{13}CN^-$ both *trans* and *cis* isomers as well as $Au(^{13}CN)_2^-$ were in fast exchange and the average resonance moved toward $Au(^{13}CN)_2^-$ resonance to an extent that *cis* complex seems to disappear as in Figure 27E. When the concentration of $^{13}CN^-$ was increased it gave a precipitate. (Note in this experiment the concentration of Au(I)cap and CN^- are higher than the first experiment which caused $Au(^{13}CN)_2^-$ to precipitate). The precipitate

was not resolved. When the precipitate was filtered and redissolved in DMSO-d_6, only one resonance at 153.67 ppm appeared which is due to $Au(^{13}CN)_2^-$ complex.

7. Cyanotri(alkyl/aryl)phosphinegold(I) Complexes

7.1. Preparation Of R_3PAuCl Complexes

Different methods were used to prepare different R_3PAuCl complexes as follows:

7.1.1. Preparation Of Ph_3PAuCl

Chloro(triphenylphosphine)gold(I) was prepared by dissolving sodium tetrachloroaurate (2.0 g; 5.0 mmol) in a 1:1 mixture of acetone and ethanol (15 ml). Triphenylphosphine (2.6 g; 10 mmol) solution in chloroform (15 ml) was added to the sodium tetrachloroaurate solution with stirring. The solution became warm, the yellow color disappeared, and a white precipitate formed. The solution was filtered, and the volume of the filtrate was reduced to 10 ml. When cooled in a refrigerator, white crystals were formed (yield is 66%) (93).

7.1.2. Preparation Of Et_3PAuCl

A solution of sodium tetrachloroaurate (2.0 g; 5.0 mmol) in (10 ml) ethanol was prepared. This solution was cooled to 0°C in an ice-bath and stirred vigorously. Triethylphosphine (1.5 ml; 10 mmol) was added slowly and carefully using a syringe. An orange precipitate was first filtered. Then the mixture was diluted with distilled water (20 ml), and left for one hour with stirring. A white product was collected, washed two times with 10 ml of distilled water, and dried overnight (yield is 72%) (94).

7.1.3. Preparation Of n-Pr_3PAuCl

To a solution of chloroauric acid (3.0 g; 8.0 mmol) in deionized water (150 ml) maintained at 0°C, a solution of 2.2'-thiodiethanol (thiodiglycol) (2.0 g; 0.016 mol) in deionized water (40 ml) was added dropwise with constant stirring. Once the mixture turned colorless, the tri-n-propylphosphine (1.3 g; 8.0 mmol; 1.6 ml) was added by a syringe. The mixture was stirred for 30 minutes at room temperature. An emulsion was formed and separated from the aqueous layer, which was cooled in a refrigerator overnight, forming pale yellow oil.

7.1.4. Preparation Of (MeEtPh)PAuCl

A solution of chloroauric acid (3.0 g; 8.0 mmol) in deionized water (250 ml) was prepared, cooled to 0°C in an ice-bath, a diluted solution of 2,2'-thiodiethanol (thiodiglycol) (2.0 g; 0.016 mol) in deionized water (40 ml) was added dropwise while stirring. As the solution turned colorless, (methylethylphenyl)phosphine ligand (1.2 g; 8.0 mmol; 1.5 ml) was added using a syringe. Stirring continued at room temperature for an additional 50 minutes. The resulting emulsion was cooled in a refrigerator overnight to give a clear yellow oil. The oil was separated from the aqueous layer by extraction with dichloroethane.

7.2. Preparation Of $R_3PAuC^{15}N$ Complexes

Labelled tri(alkyl/aryl)phosphinegold(I)cyanide complexes were prepared by adding solid $KC^{15}N$ (10% labelled and 90% unlabelled) directly to an alcoholic solution of R_3PAuCl. The method of preparation was similar for all the cyanide compounds, as an example detailed preparation for the cyanotriethylphosphinegold(I) compound is mentioned as follows:

A solution of chlorotriethylphosphinegold(I) was prepared by

dissolving 0.085 g (0.25 mmol) in 3 ml of ethanol to give a pale pink solution. An aqueous solution of (10% label) $KC^{15}N$ in 1.0 ml of deionized water was added to the ethanolic solution. This solution was stirred for 5 minutes at room temperature, then cooled in an ice-bath. The resulting crystals were filtered, washed two times with deionized water, then dried under vacuum.

Acetone was used as a solvent for chlorotriphenylphosphine and chlorotri-iso-propylphosphine because they were not soluble in ethanol.

7.3. Elemental Analysis

The elemental analysis for carbon, hydrogen and nitrogen of chlorotri(alkyl/aryl)phosphinegold(I) and label cyanotri(alkyl/aryl)-phosphinegold(I) complexes were carried out with Carlo Erba Model 1106 Elemental Analyzer. The analytical data are given in Table 14 and Table 15 along with the calculated values:

TABLE 14 Elemental Analysis of R_3PAuCl and Percentage Yield.

PR_3	Found (cal.)% C	H	%yield
PPh_3	42.9	3.01	66
	(43.66)	(3.03)	
PEt_3	21.1	4.4	72
	(20.5)	(4.3)	
$P(n\text{-}Pr)_3$	24.4	6.9	oily
	(27.5)	(5.4)	
P(MeEtPh)	28.5	3.4	oily
	(28.1)	(3.4)	

TABLE 15 Elemental Analysis of $R_3PAuC^{15}N$, Melting Points and Percentage Yield.

R	Found (cal.)% C	H	N	Found (lit.) m.pt.	%yield
Me	15.94	2.97	3.86	201	80
	(16.0)	(3.0)	(5.0)		
Et	25.08	4.54	4.16	109 (113)[80]	41
	(24.58)	(4.39)	(4.39)		
i-Pr	31.64	5.77	3.80	108	54
	(31.27)	(5.47)	(3.91)		
Ph	46.23	3.29	2.81	209 (204)[80]	90
	(46.93)	(3.08)	(3.08)		

7.4. Disproportionation Reactions Of $R_3PAuC^{15}N$ In CD_3OD

Disproportionation reactions of $R_3PAuC^{15}N$ in CD_3OD have been studied using ^{31}P and ^{15}N nuclear magnetic resonance spectroscopy as follows:

7.4.1. Disproportionation Reactions Using ^{31}P NMR Spectroscopy

Solid compounds of $Me_3PAuC^{15}N$, $Et_3PAuC^{15}N$, and $i\text{-}Pr_3PAuC^{15}N$ were directly transferred to an NMR tube where 1.0 ml of CD_3OD were added to make solutions ready for direct NMR studies. All complexes are soluble in the solvent. A solution of $Ph_3PAuC^{15}N$ (0.01 M in 1 ml CD_3OD) was also prepared in NMR tube. Because of the low solubility of $Ph_3PAuC^{15}N$ complex in methanol, a lower concentration of the complex was used. ^{31}P NMR spectra were monitored for all solutions.

Figure 28 shows the ^{31}P NMR spectra of 0.02 M Me_3PAuCN, Et_3PAuCN, $i\text{-}Pr_3PAuCN$ and 0.01 M Ph_3PAuCN complexes in CD_3OD solution. In each case two resonances of R_3PAuCN and $(R_3P)_2Au^+$ are observed as indicated in Equation 15. Note that the ratio of R_3PAuCN

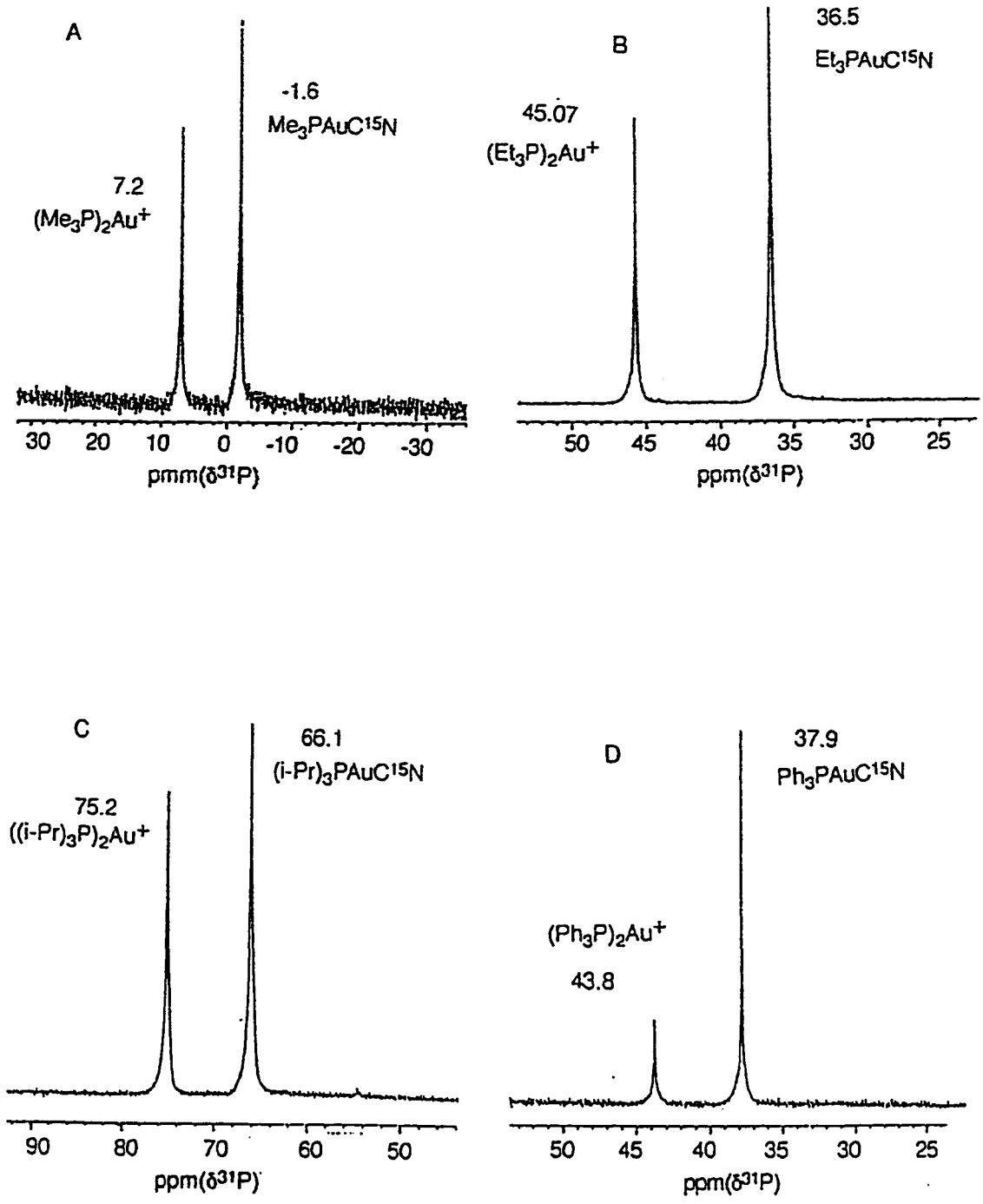

Figure 28 The 109.25 MHz ^1H noise-decoupled ^{31}P NMR spectra in CD_3OD of (A) 0.02 M $Me_3PAuC^{15}N$, (B) 0.02 M $Et_3PAuC^{15}N$, (C) 0.02 M $i\text{-}Pr_3PAuC^{15}N$ and (D) 0.01 M $Ph_3PAuC^{15}N$.

to $(R_3P)Au^+$ resonances (R = Me, Et, i-Pr and Ph) which can be monitored by NMR peaks are different for different complexes. And this is may be due to the fact that K_{eq} is different for each complex (78).

7.4.2. Disproportionation Reactions Using ^{15}N NMR

Figure 29 shows the ^{15}N NMR spectra of $Me_3PAuC^{15}N$, $Et_3PAuC^{15}N$, and $i\text{-}Pr_3PAuC^{15}N$ complexes of the same sample as have been used for the ^{31}P NMR measurements. The chemical shift difference for $i\text{-}Pr_3PAuC^{15}N$ and $Au(C^{15}N)_2^-$ probably are very close and therefore only one peak is observed. For $Me_3PAuC^{15}N$ two peaks overlapping and appearing almost as one peak was observed. However two peaks are observed for $Et_3PAuC^{15}N$ complex. These two peaks are due to $Au(C^{15}N)_2^-$ and $Et_3PAuC^{15}N$ complexes. The less intense peak at 264.0 ppm is due to $Au(C^{15}N)_2^-$ complex and more intense peak at 262.5 ppm is due to $Et_3PAuC^{15}N$ resonance (78).

For $Ph_3PAuC^{15}N$ only one peak representing ^{15}N resonance was observed at 265.5 ppm. However the signal to noise ratio was not high enough for good analysis (Figure 30).

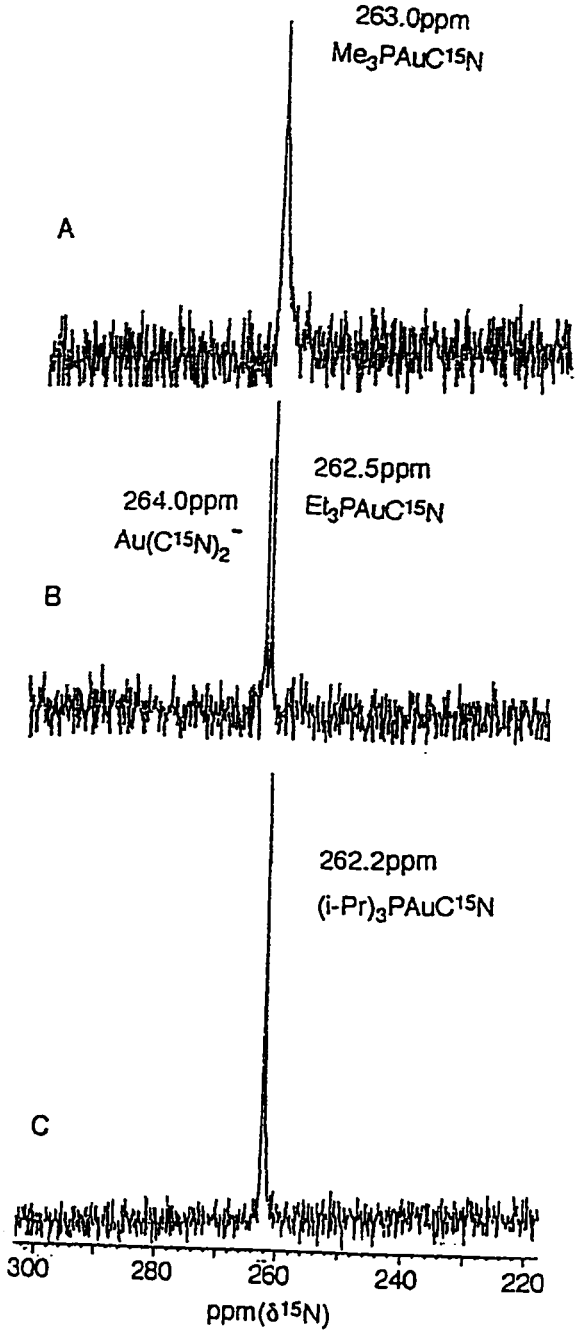

Figure 29 The 27.24 MHz ^1H noise-decoupled ^{15}N NMR spectra in CD_3OD of (A) 0.02 M $Me_3PAuC^{15}N$, (B) 0.02 M $Et_3PAuC^{15}N$ and (C) 0.02 M i-$Pr_3PAuC^{15}N$.

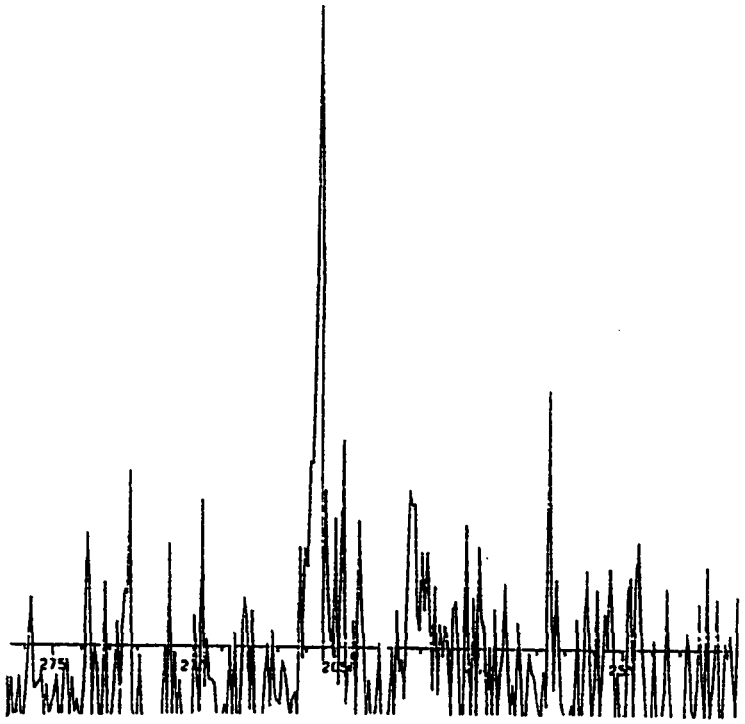

Figure 30 The 27.24 MHz ^{1}H noise-decoupled ^{15}N NMR spectra in CD_3OD of 0.01 M $Ph_3PAuC^{15}N$.

CHAPTER FOUR

DISCUSSION AND CONCLUSION

1. DISCUSSION

As described in the literature (5,8,95) when CN^- is added to gold(I)thiols, it immediately binds to this complex forming $RS\text{-}Au\text{-}CN^-$. This asymmetric gold complex is reported to disproportionate to give $Au(CN)_2^-$ and $Au(SR)_2^-$ as follows (5,8,95):

$$AuSR + HCN \;\text{<===>}\; RS\text{-}Au\text{-}CN^- + H^+ \qquad \text{(eq. 16)}$$

$$RS\text{-}Au\text{-}CN^- + HCN \;\text{<===>}\; Au(CN)_2^- + RSH \qquad \text{(eq. 17)}$$

$$AuSR + RSH \;\text{<===>}\; Au(SR)_2^- + H^+ \qquad \text{(eq. 18)}$$

$$2(RS\text{-}Au\text{-}CN^-) \;\text{<===>}\; Au(CN)_2^- + Au(SR)_2^- \qquad \text{(eq. 19)}$$

The $C^{15}N^-$ binds to gold(I) very strongly, and the formation constant of $Au(CN)_2^-$ is reported (96) as log β_2 36.6.

It is interesting to note that in both cases, tm-Au-$C^{15}N^-$ and

tg-Au-$C^{15}N^-$, the ^{15}N NMR chemical shifts are very similar ca. 260.30 ppm, which indicates that the electronic environments of CN^- ligand are very similar in both cases, which may be explained as the binding site of complexed thiols is further away.

As noted in Table 8 and Table 9, two resonances are observed for $Au(C^{15}N)_2^-$ and RS-Au-$C^{15}N^-$ species and the integration can be easily measured for both species. It is assumed that T_1 for both species are constant throughout the experiment.

It was attempted to calculate equilibrium constants for reactions 16 through 19, however the free [CN^-] concentration is extremely small and could not be determined, therefore the K_{eq} was not reported (5). In the present study, the same problem is also encountered, so the ratio of $[Au(CN)_2^-]^2$ / $[RS\text{-}Au\text{-}CN^-]^2$ (assuming $[Au(CN)_2^-] = [Au(SR)_2^-]$) was calculated and reported in Table 8 and Table 9 as to be Q. When the concentration of CN^- increases, the Q increases in both Autm and Autg cases, which indicates the dissociation of the polymer and an equilibrium shift in the direction of $Au(CN)_2^-$.

It was attempted to calculate life time of RS-Au-CN^- species on the basis of a noncoupled two-site exchange model for the system noted in equation 19. Populations of species beyond coalescence were estimated from the extrapolation of precoalescence populations. Fitting the calculated spectral data are not very satisfactory, indicating that the process involved is not a simple two-site exchange. There must be various species at equilibrium as noted in equations 16 to 19 involving multisite exchange.

The ^{15}N resonance of free $C^{15}N^-$ is not observed in any of the gold complexes. This effect has also been reported in $^{13}CN^-$ exchange studies with other gold(I) drugs (5,8,95), although the aqueous saturated free $KC^{15}N$ shows a peak at 177.8 ppm (97). Since the free $C^{15}N^-$ resonance was not observed, the concentration could not be determined. Its exchange with various gold species which exist in solution might explain the lack of an observable peak.

Another factor which introduced errors in the calculation is the uncertainty in the concentrations of these drugs. It was estimated that Autg is only 80% pure (61). For the Autm complex, it is assumed 10% free thiomalate, 0.3 mole glycerol and 2 mole water for every 1 mole of Autm (51).

It is interesting to note that at low concentrations of $C^{15}N^-$ to Autm up to 1:2 molar ratios, no $Au(C^{15}N)_2^-$ was observed (Table 8). This shows that very little disproportionation of tm-Au-$C^{15}N^-$ species occurs. However, at higher concentrations of $C^{15}N^-$, the Autm polymer breaks down and Q increases. Upon the addition of $C^{15}N^-$ to Autg, the $Au(CN)_2^-$ resonance was always observed regardless of concentration ratio. This observation is important because even for patients who are not heavy smokers, still the lower accumulation of cyanide concentration will bind to Autm or Autg forming a RS-Au-CN^- linear complex, which can also cross membranes to red blood cells. Even though for heavy smokers $Au(CN)_2^-$ is the carrier of gold to red blood cells, RS-Au-CN^-, though not as effective, is another form of carrier of gold to red blood cells for moderate smokers.

The gold(I) thiol complexes are known to form polymers, in the region of hexa- to octamers (12,15,50,91,98,99). As was observed in Figure 24A, 26A and 27A the ^{13}C NMR resonances are very broad and the solution was very viscous suggesting the formation of polymers.

The Autm in the presence of tm^- or other added thiols usually forms $Au(SR)_2^-$ complexes (52,54,61,100). As shown in Figure 24B the resonances b_1 and b_2 at 47.96 ppm and 43.57 ppm appeared at a 1:1 ratio of Au(I)cap:tm^-. At a 1:2 ratio of Au(I)cap:tm^- there was no significant change in the spectrum of 24C. These results indicate that tm^- bound to the Au(I)cap complex, but it did not displace all the captopril in the $Au(tm)_2^-$ complex. The displaced captopril is in fast exchange with gold(I) and therefore only the exchange averaged resonances are observed. These resonances may be due to the various species present as tm-Au(I)-cap^-, $Au(cap)_2^-$ etc.

As noted in Table 11 and as shown in Figure 24C, the various $-CH_3$ resonances are observed for the captopril in the presence of thiomalate. These $-CH_3$ resonances are due to the tm-Au(I)-cap^- as well as $Au(cap)_2^-$ species present in solution. However, the Au(I)cap polymer is very stable, so it will not react even with excess thiomalate and therefore the resonances for the different species could not be resolved .

When KCN was added to Au(I)cap solution, at a 1:1 ratio, the

resonances were broad, however, at a 1:2 ratio of Au(I)cap:CN^- the resonances of captopril were sharper as shown in Figure 25B. Note that the cap-Au(I)-CN^- complex at a 1:1 ratio was only soluble at pH* 12.20 however, at a 1:2 ratio the complex was soluble even at pH* 7.20, suggesting the formation of $Au(CN)_2^-$ complex which is soluble even at neutral pH* (5,8).

The equilibrium competition of HCN and thiols (RSH) for gold(I) favours cyanide and mixed ligand complexes (RS-Au-CN^-) which disproportionate to $Au(SR)_2^-$ and $Au(CN)_2^-$ species (5,8).

The two resonances observed in the 1:2 Au(I)cap:CN^- spectrum at 155.38 ppm and 154.09 ppm are due to the $Au(CN)_2^-$ and cap-Au-CN^- species (Figure 25 B and C). In the high-field region 0-70 ppm, the resonances are not well resolved. This may be due to the formation of various species which are in equilibrium as Au(I)cap, cap-Au(I)-CN^- and $Au(cap)_2^-$.

In the presence of labelled $^{13}CN^-$, it can be seen that both *trans* and *cis* Au(I)cap complex give two distinct isomers. The *trans*

cap-Au(I)-$^{13}CN^-$ resonance is low field compare to *cis* isomer. The assignment of these two resonances are based on the mole ratio of the free two isomers present in the solution (72).

In previous studies, it was found that the formation constant for the *cis* isomer is greater than that of the *trans* for CH_3Hg-captopril complex (77). In this study, it was found that *cis* cap(c)-Au-$^{13}CN^-$ resonance is higher field than *trans* cap(t)-Au-$^{13}CN^-$ resonance. This can be explained in terms of the stability of the Au-cap bond. The d_π-p_π back bonding in the cap(c)-Au-$^{13}CN^-$ is greater than cap(t)-Au-$^{13}CN^-$ which in turn will shift the $^{13}CN^-$ resonance upfield (101).

The X-ray structure of Me_3PAuCN, Et_3PAuCN, and Ph_3PAuCN shows that these complexes are monomer in solid state (80-82). However, these complexes undergo ligand scrambling reaction in solution as soon as they are dissolved (78-80) as shown in equation 15. The K_{eq} of these complexes are given in Table 16. Various factors which K_{eq} depends on have been studied (78) and these are: The nature of the solvent, the size of the ligands, initial concentration of complexes, the ionic strength of the medium etc. (78,80). Figure 28D shows the ^{31}P NMR spectrum of Ph_3PAuCN. The

K_{eq} of this complex is 0.112, therefore $(Ph_3P)_2Au^+$ resonance is much less intense compare to Ph_3PAuCN resonance. On the other hand $(Me_3P)_2Au^+$ resonance is much more intense as shown in Figure 28A compare to that of Me_3PAuCN because the K_{eq} is 0.37 for this complex (78).

TABLE 16 ^{15}N and ^{31}P NMR Chemical Shifts in ppm and K_{eq} Data for $R_3PAuC^{15}N$.

R	^{15}N R_3PAuCN	^{31}P R_3PAuCN	^{31}P $(R_3P)_2Au^+$	$(K_{eq})^{78}$	$(\theta,deg)^{78}$
Me	263.0	-1.60	7.200	0.37	118
Et	262.5	36.50	45.07	0.24	137
i-Pr	262.2	66.10	75.20	0.29	160
Ph	265.5	37.90	43.80	0.112	145

Unfortunately, the ^{15}N NMR chemical shift difference between the $Au(C^{15}N)_2^-$ and $R_3PAuC^{15}N$ were very small and therefore the peaks are not resolved, except for $Et_3PAuC^{15}N$ complex for which two resonances were observed. The assignment of $Au(C^{15}N)_2^-$ and $Et_3PAuC^{15}N$ resonances are based on K_{eq} of the complex (78) which is 0.24. Therefore $Au(C^{15}N)_2^-$ resonance should be less intense than the $Et_3PAuC^{15}N$ resonance as noted in equation 15. The broad ^{15}N resonance for $Me_3PAuC^{15}N$ shown in Figure 29A indicates that $Au(C^{15}N)_2^-$ and $Me_3PAuC^{15}N$ are exchanging slowly, however the sharpness of the $i\text{-}Pr_3PAuC^{15}N$ resonance indicates that both compounds are in fast exchange.

The ^3J for cis $[Mo(N_2)_2(PMe_2Ph)_4](thf)$ is reported to be 0.9 Hz (102) however, no ^3J coupling for any $^{31}P\text{-}Au\text{-}C\text{-}^{15}N$ complex studied here was observed. The ^2J coupling ($^{15}N\text{-}^{31}P$) for $R_3P\text{-}Au(^{15}N\text{-}$phthalimide) where R = Me, Et, Ph, i-Pr etc. were monitored (103) and found to be in the following order Me > Et > i-Pr.

From Me to i-Pr, the phosphorus cone angle (104) increases (Table 16) consequently the s character on the phosphorus lone pair decrease and therefore a weaker P-Au σ bond is expected. Which

means that Au-CN σ bond will be stronger. For Ph_3P-Au-CN the K_{eq} is smaller and for Me_3PAuCN is higher (Table 16). The disproportionation for Ph_3P-Au-CN complex is less than that of Me_3PAuCN.

It should be noted here that in previous studies, only one ^{31}P resonance for Ph_3PAuCN complex at 297 K was found (78,80,105) however at low temperature 200 K, two resonances for $(Ph_3P)_2Au^+$ and Ph_3PAuCN were observed. Contrary to this observation, in the present study two resonances are observed even at room temperature, although similar concentration and NMR frequency is used in both studies.

2. Conclusions

On the basis of the above investigations the following conclusions are drawn:

1. ^{15}N and ^{13}C NMR techniques are very useful tools for studying the interaction of cyanide ion with gold(I)thiolate complexes because the spectra are simple, giving only few resonances for a given system.

2. When cyanide ion interacts with Au(I)thiolate complexes, aurocyanide complex, $[Au(CN)_2^-]$, is the major product at a ratio of Au(I)thiolate:CN^- greater than or equal two. At lower ratios a mixed ligand complex, $[RSAuCN]^-$, is also produced.

3. From ^{15}N NMR spectra, approximate lifetime of the RS-Au-CN^- species has been calculated. It shows that as the concentration of CN^- increases in solution the disproportionation reaction of RS-Au-CN^- species to $Au(CN)_2^-$ and $Au(SR)_2^-$ also increases.

4. For the first time a crystalline gold(I) thiolate complex has been isolated.

5. Gold(I)captopril complex at 1:1 ratio was synthesized and forms a high molecular weight polymer in aqueous solution.

6. Both thiomalate and CN^- binds to Au(I)cap complex, but CN^- binds more strongly than thiomalate. Based on the ^{13}C NMR chemical shifts, the *cis* cap(c)-Au-$^{13}CN^-$ isomer is found to be

more stable than the *trans.* isomer.

7. ^{15}N label cyanotri(alkyl/aryl)phosphinegold(I) ($R_3PAuC^{15}N$) complexes were prepared. In solution these complexes disproportionate to give $(R_3P)_2Au^+$ and $Au(CN)_2^-$. The disproportionation reactions of these complexes shown to be affected by the steric hindrance of phosphine ligands.

8. Since RS-Au-CN^- was not isolated, and a mixture of RS-Au-CN^-, $Au(SR)_2^-$ and $Au(CN)_2^-$ are always observed in solution, this led to the conclusion that RS-Au-CN^- is always in equilibrium with $Au(SR)_2^-$ and $Au(CN)_2^-$.

9. The ^{15}N NMR chemical shift range for all the $R_3PAuC^{15}N$ species is 262.2-265.5 ppm in CD_3OD. The ^{15}N NMR chemical shift range for RS-Au-$C^{15}N^-$ and R_3P-Au-$C^{15}N$ is between 260-265 ppm. Which indicates that ^{15}N NMR chemical shift is insensitive to the type of ligand attached to gold(I).

References

1. W. J. Jusko, *J. Pharmacokin. Biopharm.*, 6(1), 7 (1978).

2. P. W. Darby and J. Wilson, *Br. J. Ophthalmol.*, 51, 366 (1967).

3. D. H. Brown and W. E. Smith, *Chem. Soc. Rev.*, 9, 217 (1980).

4. C. F. Shaw III, *Comments Inorg. Chem.*, 8, 233 (1989).

5. G. G. Graham, J. R. Bales, M. C. Grootveld and P. J. Sadler, *J. Inorg. Biochem.*, 25, 163 (1985).

6. A. A. Isab, A. L. Hormann, M. T. Coffer and C. F. Shaw III, *J. Amer. Chem. Soc.*, 110, 3278 (1988).

7. A. A. Isab, *J. Inorg. Biochem.*, 45, 1 (1992).

8. G. Lewis and C. F. Shaw III, *Inorg. Chem.*, 25, 58 (1986).

9. G. G. Graham, T. M. Haavisto, H. M. Jones and G. D. Champion, *Biochem. Pharmacol.*, 33, 1257 (1984).

10. D. W. James, N. W. Ludvigsen, L. G. Cleland and S. C. Milazzo, *J. Rheum.*, 9, 532 (1982).

11. D. Lewis, H. A. Capell, C. J. McNiel, M. S. Iqbal, D. H. Brown, W. E. Smith, *Ann. Rheum. Dis.*, 42, 566 (1983).

12. C. F. Shaw III, *Inorg. Perspect. Biol. Med.*, 2, 287 (1979).

13. W. E. Spiar, A. H. Sommer and J. G. White, *Phys. Rev.*, 115, 57 (1959).

14. J. Knecht, P. Fischer, H. Overhoff and F. Hensel, *J. Chem. Soc. Chem. Commun.*, 905 (1978).

15. P. J. Sadler, *Struct. Bonding* (Berlin), 29, 171 (1976).

16. H. Schmidbaur, *Angew. Chem. Int. Ed. Engl.*, 15(12), 728 (1976).

17. R. J. Puddephatt, *The Chemistry of Gold*, Elsevier, Amsterdam, (1978).

18. K. Leary, A. Zalkin and N. Bartlett, *Inorg. Chem.*, 13, 775 (1974).

19. P. G. Jones, A. G. Maddock, M. J. Mays, M. M. Muir and A. F. Williams, *J. Chem. Soc. Dalton Trans.*, 1434 (1977).

20. L. J. Guggenberger, *J. Organomet. Chem.*, 81, 271 (1974).

21. N. C. Baenziger, K. T. Dittmore and J. R. Doyle, *Inorg. Chem.*, 13, 805 (1974).

22. E. L. Meutterties and C. W. Alegranti, *J. Amer. Chem. Soc.*, 92, 4114 (1970).

23. L. Malatesta, L. Naldini, G. Simonetta and F. Cariati, *Coord. Chem. Rev.*, 1, 255 (1966).

24. P. G. Jones, J. J. Guy and G. M. Sheldrick, *Acta Cryst.*, B31, 2687 (1975).

25. M. R. Caira, L. R. Nassimbeni and A. L. Rodgers, *Acta Cryst.*, B31, 1112 (1975).

26. S. Komiya, J. C. Huffman and J. K. Kochi, *Inorg. Chem.*, 16, 1253 (1977).

27. E. S. Clark, D. H. Templeton and C. M. McGillavry, *Acta Cryst.*, 11, 284 (1958).

28. V. F. Duckworth and N. C. Stephenson, *Inorg. Chem.*, 8, 1661 (1969).

29. R. Timkovich and A. Tulinsky, *Inorg. Chem.*, 16, 962 (1977).

30. W. T. Robinson and E. Sinn, *J. Chem. Soc. Dalton Trans.*, 726 (1975).

31. N. Farrell, *Transition Metal Complexes as Drugs and Chemotherapeutic Agents*, Kluwer Acad. Publisher, U.S.A, (1989).

32. W. D. Block, O. H. Buchanan and R. H. Freyberg, *J. Pharm. Exp. Ther.*, 73, 200 (1941).

33. W. D. Block, O. H. Buchanan and R. H. Freyberg, *J. Pharm. Exp. Ther.*, 74, 355 (1942).

34. J. S. Lawrence, *Ann. Rheum. Dis.*, 20, 341 (1961).

35. R. H. Freyberg, W. D. Block and S. Levy, *Ann. Rheum. Dis.*, 1, 77 (1942).

36. P. M. Smith, E. M. Smith and N. L. Gottlieb, *J. Lab. Clin. Med.*, 82, 930 (1973).

37. E. S. Botzvadza, L. M. Movlishvili, N. E. Kuchava and E. N. Ghinturi, *Phys. Med. Biol.*, 14, 19 (1969).

38. R. C. Gerber, H. E. Paulus, R. Bluestone and M. Lederer, *Arthr. Rheum.*, 15, 622 (1972).

39. R. H. Freyberg, W. D. Block and S. Levey, *J. Clin. Invest.*, 20, 401 (1941).

40. E. G. McQueen and P. W. Dykes, *Ann. Rheum. Dis.*, 28, 437 (1969).

41. E. A. Tonna, G. Brecker, E. P. Cronkite and I. L. Schwartz, *Arthr. Rheum.*, 6, 1 (1963).

42. N. L. Gottlieb, P. M. Smith and E. M. Smith, *Arthr. Rheum.*, 15, 16 (1972).

43. R. Grahame, R. Billings, M. Laurance, V. Marks and P. J. Wood, *Ann. Rheum. Dis.*, 33, 536 (1974).

44. H. Nakamura and M. Igarishi, *Ann. Rheum. Dis.*, 36, 209 (1977).

45. A. F. Oryschak and F. N. Ghadially, *Virchows Arch. B. Cell Pathol.*, 20, 29 (1976).

46. A. F. Oryschak and F. N. Ghadially, *J. Pathol.*, 119, 183 (1976).

47. F. N. Ghadially, A. F. Oryschak and D. M. Mitchell, *Ann. Rheum. Dis.*, 35, 67 (1976).

48. B. Vernon-Roberts, J. L. Dore, J. D. Jessop and W. J. Henderson, *Ann. Rheum. Dis.*, 35, 477 (1976).

49. W. E. Smith and J. Reglinski, *Perspect. Bioinorg. Chem.*, 1, 183 (1991).

50. A. A. Isab and P. J. Sadler, *J. Chem. Soc. Dalton Trans.*, 1657 (1981).

51. M. C. Grootveld, M. T. Razi and P. J. Sadler, *Clin. Rheumatol.*, 3 (suppl. 1), 5 (1984).

52. A. A. Isab and P. J. Sadler, *J. Chem. Soc. Dalton Trans.*, 135 (1982).

53. M. T. Razi, G. Otiko and P. J. Sadler, Ligand Exchange Reactions of Gold Drugs in Model Systems and in Red Cells (Platinum,

Gold, and Other Metal Chemotherapeutic Agents, ACS Symposium Series v. 209, Ed. S. J. Lippard), p. 371. ACS, Washington (1983).

54. A. A. Isab and P. J. Sadler, *J. Chem. Soc. Chem. Comm.*, 1051 (1976).

55. A. A. Isab, *J. Inorg. Biochem.*, 45, 261 (1992).

56. J. J. Pesek and W. R. Mason, *Inorg. Chem.*, 18, 924 (1979).

57. M. D. Rhodes, P. J. Sadler, M. D. Scawen and S. Silver, *J. Inorg. Biochem.*, 46, 129 (1992).

58. A. K. H. Al-Sa'ady, K. Moss, C. A. McAuliffe and R. V. Parish, *J. Chem. Soc. Dalton Trans.*, 1609 (1984).

59. R. J. Fessenden and J. S. Fessenden, *Organic Chemistry*, Willard Grant, Boston, p. 815 (1982).

60. L. F. Johnson and W. C. Jankowski, *Carbon-13 NMR Spectra*, Wiley Interscience, New York, p. 197 (1972).

61. C. F. Shaw III, J. Eldridge and M. P. Cancaro, *J. Inorg. Biochem.*, 14, 267 (1981).

62. S. H. Ferreira, D. C. Bartelt and L. J. Greene, *Biochem.*, 9, 2583 (1970).

63. H. Gavras, H. R. Brunner, J. H. Laragh, I. Gavras and R. A. Vukovich, *Clin. Sci. Mol. Med.*, 48, 57s (1975).

64. H. R. Brunner, H. Gavras, B. Waeber, G. R. Kershaw, G. A. Turini, R. A. Vukovich, D. N. McKinstry and I. Gavras, *Ann. Intern. Med.*, 90, 19 (1979).

65. R. C. Heel, R. N. Brogden, T. M. Speight and G. S. Avery, *Drugs*, 20, 409 (1980).

66. H. R. Brunner, H. Gavras, B. Waeber, S. C. Textor, G. A. Turini and J. P. Wauters, *Hypertension*, 2, 558 (1980).

67. D. B. Case, S. A. Atlas, P. A. Sullivan and J. H. Laragh, *Circulation*, 64, 765 (1981).

68. M. F. R. Martin, F. McKenna, H. A. Bird, K. E. Surrall, J. S. Dixon and V. Wright, *Lancet*, I, 1325 (1984).

69. V. Madison and J. Schellman, *Biopolymers*, 9, 511 (1970).

70. J. T. Gerig, *Biopolymers*, 10, 2435 (1971).

71. C. A. Evans and D. L. Rabenstein, *J. Amer. Chem. Soc.*, 96, 7312 (1974).

72. D. L. Rabenstein and A. A. Isab, *Anal. Chem.*, 54, 526 (1982).

73. S. Mizushima, *Adv. Protein Chem.*, 9, 299 (1954).

74. M. A. Hughes, G. L. Smith and D. R. Williams, *Inorg. Chim. Acta.*, 107, 247 (1985).

75. G. L. Christie, M. A. Hughes, S. B. Rees and D. R. Williams, *Inorg. Chim. Acta.*, 151, 215 (1988).

76. A. A. Isab, *J. Inorg. Biochem.*, 30, 69 (1987).

77. A. A. Isab, *J. Chem. Soc. Dalton Trans.*, 449 (1991).

78. A. L. Hormann-Arendt and C. F. Shaw III, *Inorg. Chem.*, 29, 4683 (1990).

79. M. M. El-Etri and W. M. Scovell, *Inorg. Chem.*, 29, 480 (1990).

80. A. L. Hormann, C. F. Shaw III, D. W. Bennett and W. M. Reiff, *Inorg. Chem.*, 25, 3953 (1986).

81. S. Ahrland, B. Aurivillius, K. Dreisch, B. Noren and A. Oskarsson, *Acta. Chem. Scand.*, 46, 262 (1992).

82. P. Jones and J. Lautner, *J. Acta Crystallogr., Sect.* C44, 2091 (1988).

83. C. A. McAuliffe, R. V. Parish and P. D. Randall, *J. Chem. Soc. Dalton Trans.*, 1426 (1977).

84. P. F. Barron, L. M. Engelhardt, P. C. Healy, J. Oddy and A. H. White, *Aust. J. Chem.*, 40, 1545 (1987).

85. S. Al-Baker, W. E. Hill and C. A. McAuliffe, *J. Chem. Soc. Dalton Trans.*, 1297 (1986).

86. M. J. Mays and P. A. Vergano, *J. Chem. Soc. Dalton Trans.*, 1112 (1979).

87. R. V. Parish, O. Parry and C. A. McAuliffe, *J. Chem. Soc. Dalton Trans.*, 2098 (1981).

88. The NMR program library, The Science and Engineering Research Council, Daresbury Lab., Cheshire, U. K.

89. P. R. Srinivasan and R. L. Lichter, *J. Magn. Resonance*, 28, 227 (1977).

90. A. A. Isab, C. F. Shaw III, J. D. Hoeschele and J. Locke, *Inorg. Chem.*, 27, 3588 (1988).

91. D. T. Hill, B. M. Sutton, A. A. Isab, T. Razi, P. J. Sadler, J. M. Trooster and G. H. M. Callis, *Inorg. Chem.*, 22, 2936 (1983).

92. R. L. Shriner, R. C. Fuson, D. Y. Curtin and T. C. Morrill, *The Systematic Identification of Organic Compounds*, J. Wiley, New York, P.121 (1980).

93. C. A. McAuliffe, R. V. Parish and P. D. Randall, *J. Chem. Soc. Dalton Trans.*, 1730 (1979).

94. F. G. Mann, A. F. Wells and D. Purdie, *J. Chem. Soc.*, 1828 (1937).

95. A. A. Isab, *J. Inorg. Biochem.*, 46, 145 (1992).

96. R. D. Hancock, N. P. Finkelstein, and A. J. Avers, *Inorg. Nucl. Chem.*, 34, 3747 (1972).

97. M. Witanowski, L. Stefaniak, S. Szymanski and H. Januszewski, *J. Magn. Resonance*, 28, 217 (1977).

98. D. H. Brown, G. McKlinley and W. E. Smith, *J. Chem. Soc. Dalton Trans.*, 1874 (1977).

99. L. F. Larkworthy and D. Sattari, *J. Inorg. Nucl. Chem.*, 42, 551 (1980).

100. C. F. Shaw III, G. Schmitz, H. O. Thompson and P. J. Witkiewicz, *J. Inorg. Biochem.*, 10, 317 (1979).

101. K. L. Brown and S. Satyanarayana, *Inorg. Chem.*, 31, 1366 (1992).

102. J. Chatt, M. E. Fakley, R. L. Richards, J. Mason and I. A. Stenhouse, *J. Chem. Research (S)*, 44 (1979).

103. S. J. Berners Price, M. J. Dimartino, D. T. Hill, R. Kuroda, M. A. Mazid and P. J. Sadler, *Inorg. Chem.*, 24, 3425 (1985).

104. C. A. Tolman, *Chem. Rev.*, 77, 313 (1977).

105. F. Cariati, D. Galizzioli and L. Naldini, *Chim. Ind. (Milan)*, 52, 995 (1970).